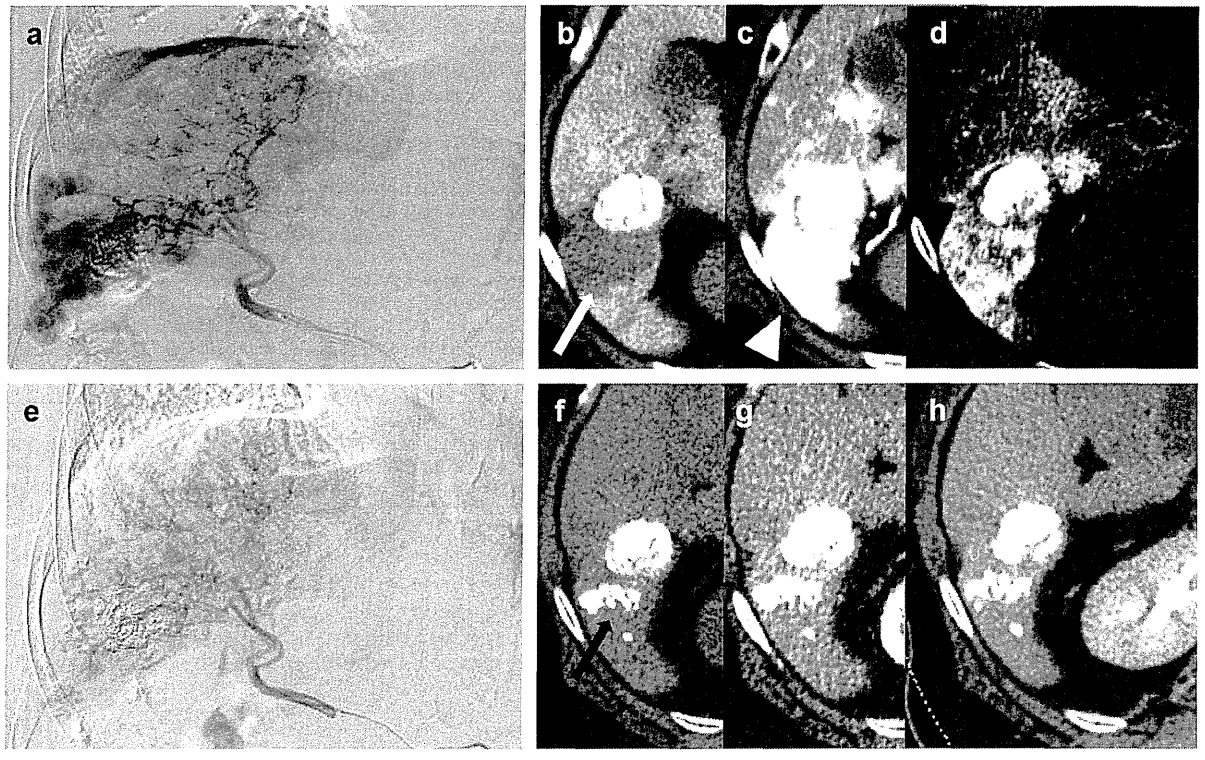

Figure 3 Representative images of tumour from case 9 showing partial response after administration of DDP-H TAC and miriplatin-TOCE. Before treatment: **a**, right hepatic angiography; **b**, computed tomography during arterial portography (CTAP). White arrow indicates tumour defect on CTAP; **c**, early phase of CT hepatic arteriography (CTHA); **d**, delayed phase of CTHA. White arrowheads indicate staining of tumour. Two months after treatment: **e**, right hepatic angiography; **f**, plain CT image; **g**, early phase of dynamic CT; **h**, delayed phase of dynamic CT. Black arrow indicates remaining lipiodol.

of DDP-H and miriplatin in combination therapy is the maximum monotherapy dose. No evidence of systemic platinum release from miriplatin-TOCE was recorded, as expected. Reflecting a possible higher disease control rate and PR response, a phase II randomised prospective study is now ongoing to investigate the efficacy of this combined therapy in a larger cohort.

Competing Interests

The authors declare that they do not have a current financial arrangement or affiliation with any organisation that may have a direct interest in their work.

Author's contributions

KK wrote manuscript and performed research. TS designed a research and wrote manuscript. YT, MT, MI, HK, and SY performed research including the angiography. TY analysed data. MN and YA designed and analysed all data. *All authors read and approved the final manuscript.*

Disclosure

The authors declare that they do not have a current financial arrangement or affiliation with any organisation that may have a direct interest in their work.

Acknowledgements

This study was supported by a grant from the Niigata University Medical and Dental Hospital (Clinical research support project/2012) to T.S.

Received: 14 May 2012 Accepted: 17 September 2012
Published: 20 September 2012

References

1. Llovet JM, Burroughs A, Bruix J: **Hepatocellular carcinoma.** *Lancet* 2003, **362**:1907–1917.
2. Villanueva A, Llovet JM: **Targeted therapies for hepatocellular carcinoma.** *Gastroenterology* 2011, **140**:1410–1426.
3. Marelli L, Stigliano R, Triantos C, Senzolo M, Cholongitas E, Davies N, Tibballs J, Meyer T, Patch DW, Burroughs AK: **Transarterial therapy for hepatocellular carcinoma: which technique is more effective? A systematic review of cohort and randomized studies.** *Cardiovasc Intervent Radiol* 2007, **30**:6–25.
4. Lencioni R: **Loco-regional treatment of hepatocellular carcinoma.** *Hepatology* 2010, **52**:762–773.
5. Ishikawa T: **Future perspectives on the treatment of hepatocellular carcinoma with cisplatin.** *World J Hepatol* 2009, **1**:8–16.
6. Llovet JM, Bruix J: **Systematic review of randomized trials for unresectable hepatocellular carcinoma: Chemoembolization improves survival.** *Hepatology* 2003, **37**:429–442.
7. Llovet JM, Real MI, Montana X, Planas R, Coll S, Aponte J, Ayuso C, Sala M, Muchart J, Sola R, Rodes J, Bruix J: **Arterial embolisation or chemoembolisation versus symptomatic treatment in patients with unresectable hepatocellular carcinoma: a randomised controlled trial.** *Lancet* 2002, **359**:1734–1739.
8. Oliveri RS, Wetterslev J, Gluud C: **Transarterial (chemo)embolisation for unresectable hepatocellular carcinoma.** *Cochrane Database Syst Rev* 2011, **16**:CD004787.
9. Varela M, Real MI, Burrel M, Forner A, Sala M, Brunet M, Ayuso C, Castells L, Montana X, Llovet JM, Bruix J: **Chemoembolization of hepatocellular**

carcinoma with drug eluting beads: efficacy and doxorubicin pharmacokinetics. *J Hepatol* 2007, **46**:474–481.
10. Groupe dEtude et de Traitement du Carcinome Hepatocellulaire: **A comparison of lipiodol chemoembolization and conservative treatment for unresectable hepatocellular carcinoma. Groupe d'Etude et de Traitement du Carcinome Hepatocellulaire.** *N Engl J Med* 1995, **332**:1256–1261.
11. Chan AO, Yuen MF, Hui CK, Tso WK, Lai CL: **A prospective study regarding the complications of transcatheter intraarterial lipiodol chemoembolization in patients with hepatocellular carcinoma.** *Cancer* 2002, **94**:1747–1752.
12. Okusaka T, Kasugai H, Shioyama Y, Tanaka K, Kudo M, Saisho H, Osaki Y, Sata M, Fujiyama S, Kumada T, Sato K, Yamamoto S, Hinotsu S, Sato T: **Transarterial chemotherapy alone versus transarterial chemoembolization for hepatocellular carcinoma: a randomized phase III trial.** *J Hepatol* 2009, **51**:1030–1036.
13. Yoshikawa M, Ono N, Yodono H, Ichida T, Nakamura H: **Phase II study of hepatic arterial infusion of a fine-powder formulation of cisplatin for advanced hepatocellular carcinoma.** *Hepatol Res* 2008, **38**:474–483.
14. Kinami Y, Miyazaki I: **The superselective and the selective one shot methods for treating inoperable cancer of the liver.** *Cancer* 1978, **41**:1720–1727.
15. Nagasue N, Yukaya H, Okamura J, Kuroda C, Kubo Y, Hirai K, Tanikawa K, Okita K, Ando K, Tamura K: **Intra-arterial administration of epirubicin in the treatment of non-resectable hepatocellular carcinoma. Epirubicin Study Group for Hepatocellular Carcinoma.** *Gan To Kagaku Ryoho* 1986, **13**:2786–2792.
16. Kishimoto S, Noguchi T, Yamaoka T, Fukushima S, Takeuchi Y: **Antitumor effects of a novel lipophilic platinum complex (SM-11355) against a slowly-growing rat hepatic tumor after intra-hepatic arterial administration.** *Biol Pharm Bull* 2000, **23**:344–348.
17. Shimakura J, Fujimoto K, Komuro S, Nakano M, Kanamaru H: **Long-term disposition of a novel lipophilic platinum complex SM-11355 in dog after intrahepatic arterial administration: highly sensitive detection of platinum and radioactivity.** *Xenobiotica* 2002, **32**:399–409.
18. Kishimoto S, Ohtani A, Fukuda H, Fukushima S, Takeuchi Y: **Relation between intracellular accumulation and cytotoxic activity of cis-[((1R, 2R)-1, 2-cyclohexanediamine-N, N')bis(myristato)]platinum(II) suspended in Lipiodol.** *Biol Pharm Bull* 2003, **26**:683–686.
19. Hanada M, Baba A, Tsutsumishita Y, Noguchi T, Yamaoka T, Chiba N, Nishikaku F: **Intra-hepatic arterial administration with miriplatin suspended in an oily lymphographic agent inhibits the growth of tumors implanted in rat livers by inducing platinum-DNA adducts to form and massive apoptosis.** *Cancer Chemother Pharmacol* 2009, **64**:473–483.
20. Hanada M, Baba A, Tsutsumishita Y, Noguchi T, Yamaoka T: **Intra-hepatic arterial administration with miriplatin suspended in an oily lymphographic agent inhibits the growth of human hepatoma cells orthotopically implanted in nude rats.** *Cancer Sci* 2009, **100**:189–194.
21. Hanada M, Takasu H, Kitaura M: **Acquired resistance to miriplatin in rat hepatoma AH109A/MP10 is associated with increased Bcl-2 expression, leading to defects in inducing apoptosis.** *Oncol Rep* 2010, **24**:1011–1018.
22. Fujiyama S, Shibata J, Maeda S, Tanaka M, Noumaru S, Sato K, Tomita K: **Phase I clinical study of a novel lipophilic platinum complex (SM-11355) in patients with hepatocellular carcinoma refractory to cisplatin/lipiodol.** *Br J Cancer* 2003, **89**:1614–1619.
23. Okusaka T, Okada S, Nakanishi T, Fujiyama S, Kubo Y: **Phase II trial of intra-arterial chemotherapy using a novel lipophilic platinum derivative (SM-11355) in patients with hepatocellular carcinoma.** *Invest New Drugs* 2004, **22**:169–176.
24. Nishikawa H, Inuzuka T, Takeda H, Nakajima J, Sakamoto A, Henmi S, Ishikawa T, Saito S, Kita R, Kimura T, Osaki Y, Koshikawa Y: **A case of advanced hepatocellular carcinoma with portal vein tumor thrombus refractory to epirubicin that showed marked decrease in tumor markers after transcatheter arterial infusion with miriplatin.** *Case Rep Oncol* 2011, **4**:327–335.
25. Court WS, Order SE, Siegel JA, Johnson E, DeNittis AS, Principato R, Martz K, Zeiger LS: **Remission and survival following monthly intraarterial cisplatinum in nonresectable hepatoma.** *Cancer Invest* 2002, **20**:613–625.
26. Niguma T, Mimura T, Tutui N: **Adjuvant arterial infusion chemotherapy after resection of hepatocellular carcinoma with portal thrombosis: a pilot study.** *J Hepatobiliary Pancreat Surg* 2005, **12**:249–253.
27. Eisenhauer EA, Therasse P, Bogaerts J, Schwartz LH, Sargent D, Ford R, Dancey J, Arbuck S, Gwyther S, Mooney M, Rubinstein L, Shankar L, Dodd L, Kaplan R, Lacombe D, Verweij J: **New response evaluation criteria in solid tumours: revised RECIST guideline (version 1.1).** *Eur J Cancer* 2009, **45**:228–247.
28. Llovet JM, Ricci S, Mazzaferro V, Hilgard P, Gane E, Blanc JF, de Oliveira AC, Santoro A, Raoul JL, Forner A, Schwartz M, Porta C, Zeuzem S, Bolondi L, Greten TF, Galle PR, Seitz JF, Borbath I, Haussinger D, Giannaris T, Shan M, Moscovici M, Voliotis D, Bruix J: **Sorafenib in advanced hepatocellular carcinoma.** *N Engl J Med* 2008, **359**:378–390.
29. Watanabe S, Nitta N, Ohta S, Sonoda A, Otani H, Tomozawa Y, Nitta Seko A, Tsuchiya K, Tanka T, Takahashi M, Murata K: **Comparison of the Anti-tumor Effects of Two Platinum Agents (Miriplatin and Fine-Powder Cisplatin).** *Cardiovasc Intervent Radiol* 2012, **35**:399–405.

doi:10.1186/1471-230X-12-127
Cite this article as: Kamimura *et al.*: Phase I study of miriplatin combined with transarterial chemotherapy using CDDP powder in patients with hepatocellular carcinoma. *BMC Gastroenterology* 2012 **12**:127.

ELSEVIER

Magnetic Compression Anastomosis for Bile Duct Stenosis After Donor Left Hepatectomy: A Case Report

H. Oya, Y. Sato, E. Yamanouchi, S. Yamamoto, Y. Hara, H. Kokai, T. Sakamoto, K. Miura, K. Shioji, Y. Aoyagi, and K. Hatakeyama

ABSTRACT

Magnetic compression anastomosis (MCA) provides a minimally invasive treatment creating a nonsurgical, sutureless enteric anastomosis in conjunction with an interventional radiologic technique by using 2 high-power magnets. Recently, the MCA technique has been applied to bile duct strictures after living donor liver transplantation or major hepatectomy. Herein we described use of MCA for bile duct stenosis 5 months after donor left hepatectomy in a 24-year-old man who presented with a stricture at the porta hepatis and intrahepatic bile duct dilatation. Unsuccessful transpapillary biliary drainage and balloon dilatation through a percutaneous transhepatic biliary drainage (PTBD) route led to the MCA. A 4-mm-diameter cylindrical samarium-cobalt (Sm-Co) daughter magnet with a long nylon wire was placed at the superior site of the obstruction through the PTBD route. A 5-mm-diameter Sm-Co parent magnet with an attached nylon handle was endoscopically inserted into the common bile duct and placed at the inferior site of obstruction. The 2 magnets were attracted, sandwiching the stricture and establishing a reanastomosis. In conclusion, the MCA technique was a unique procedure for choledochocholedochostomy in a patient with bile duct stenosis after donor hepatectomy.

BILE duct stenosis after leakage of a stump is a serious surgical complication of donor hepatectomy. Several interventions have been described to resolve the stenosis: reoperation, interventional radiology, and endoscopic therapy. Magnetic compression anastomosis (MCA) using 2 high-power magnets provides a minimally invasive treatment by creating a nonsurgical, sutureless enteric anastomosis in conjunction with an interventional radiologic technique. Recently, the MCA technique has been applied to bile duct strictures after living donor liver transplantation (LDLT) or major hepatectomy.[1,2] We have described herein a successful case of MCA for bile duct stenosis after donor left hepatectomy.

CASE REPORT

A 24-year-old man had undergone a donor left hepatectomy for his mother's liver transplantation. He subsequently suffered leakage at the bile duct stump, which resolved after percutaneous abdominal and endoscopic nasobiliary drainages. He began to experience fever with slight elevation of transaminases (aspartate aminotransferase, 79 IU/L; alanine aminotransferase, 109 IU/L) and total bilirubin (1.2 mg/dL) at 5 months after the hepatectomy. Magnetic resonance cholangiopancreatography revealed a biliary stricture at the porta hepatis with intrahepatic bile duct dilatation of the B5, B6, and B7 branches (Fig 1A). We attempted transpapillary biliary drainage, but the intrahepatic bile duct was invisible by endoscopic retrograde cholangiography except for the B8 bile duct (Fig 1B). Balloon dilatation through the percutaneous transhepatic biliary drainage (PTBD) route was impossible because the guidewire could not pass the stenotic segment (Fig 1C).

Therefore, we performed MCA after obtaining written informed consent. As preparation for the procedure, the PTBD tube was dilated to 16 French. First, a 14-French sheath tube was inserted through the dilated PTBD fistula. A 4-mm-diameter cylindrical samarium-cobalt (Sm-Co) daughter magnet with a long nylon wire was placed at the superior site of the obstruction through the sheath tube. The Papilla of Vater was enlarged using endoscopic

From the Division of Digestive and General Surgery (H.O., Y.S., S.Y., Y.H., H.K., T.S., K.M., K.H.), Gastroenterology and Hepatology (K.S., Y.A.), Niigata University Graduate School of Medical and Dental Sciences, Niigata, and Department of Radiology (E.Y.), Yokohama Seibu Hospital, St. Marianna University, Yokohama, Japan.

Address reprint requests to Hiroshi Oya, MD, Division of Digestive and General Surgery, Niigata University Graduate School of Medical and Dental Sciences, 1-757 Asahimachi-dori, Chuo-ku, Niigata, 951-8510 Japan. E-mail: h-oya@med.niigata-u.ac.jp

0041-1345/12/$–see front matter
doi:10.1016/j.transproceed.2012.01.021

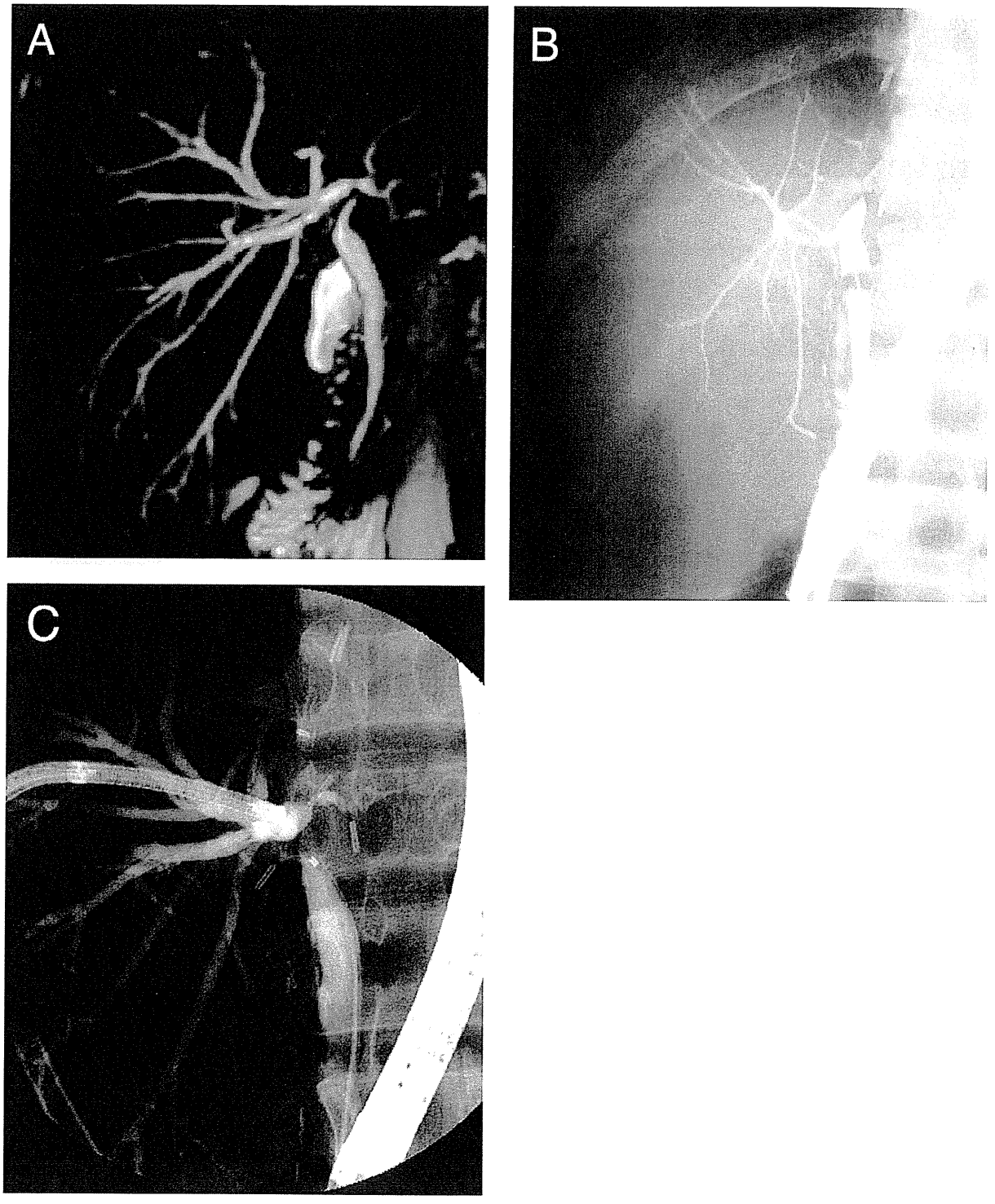

Fig 1. **(A)** Magnetic resonance cholangiopancreatography revealed a biliary stricture at the porta hepatis and intrahepatic bile duct dilatation of the B5, B6, and B7 branches. **(B)** Intrahepatic bile duct was invisible by endoscopic retrograde cholangiography except for the B8 bile duct. **(C)** Balloon dilatation through the PTBD route was impossible because the guidewire could not pass the stenotic segment.

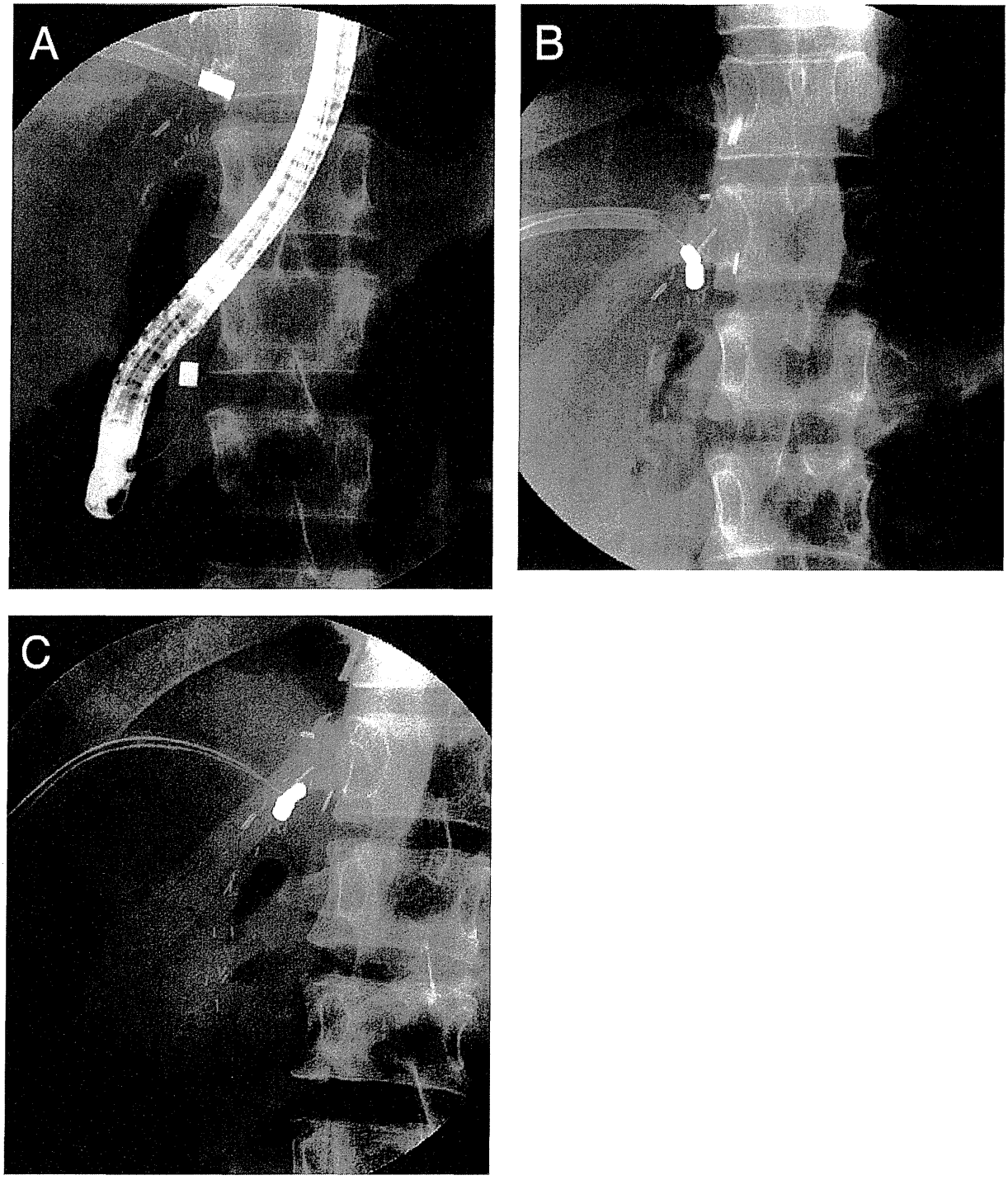

Fig 2. **(A)** A 4-mm-diameter cylindrical Sm-Co daughter magnet with a long nylon wire was placed at the superior site of the obstruction through the sheath tube. Then, a 5-mm-diameter Sm-Co parent magnet with a nylon handle attached was endoscopically inserted into the common bile duct. **(B)** The parent magnet was placed at the inferior site of obstruction. **(C)** The 2 magnets were attracted to each other magnetically, sandwiching the stricture.

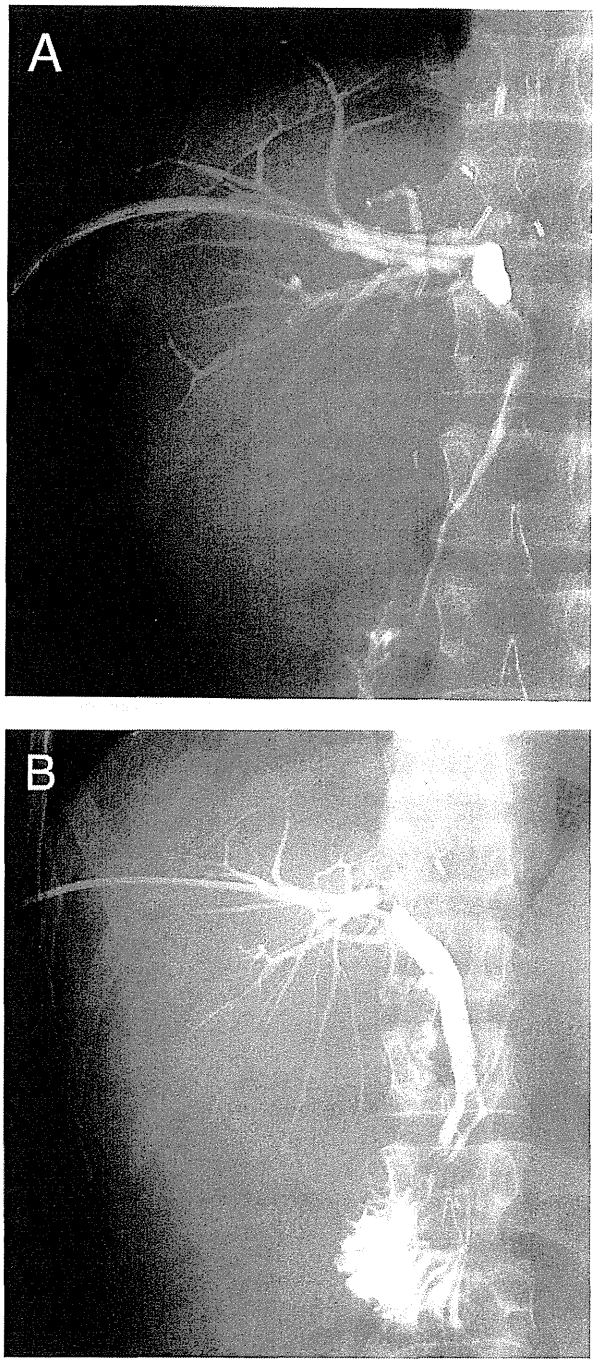

Fig 3. **(A)** Establishment of the reanastomosis was confirmed using radiological examinations. **(B)** A 12-French internal stent tube was placed at the common bile duct through the created fistula.

balloon dilation. A 5-mm-diameter Sm-Co parent magnet with a nylon handle attached endoscopically inserted into the common bile duct was placed at the inferior site of the obstruction (Fig 2A and 2B). The 2 magnets were attracted, sandwiching the stricture (Fig 2C). Establishment of the reanastomosis was confirmed by day 60 using radiological examinations (Fig 3A). Finally, a 12-French internal stent was placed in the common bile duct through the created fistula (Fig 3B). The stent tube was removed 8 months after creation of the fistula.

DISCUSSION

Donor safety is a critical issue in LDLT. Biliary complications, a major concern among LDLT donors, have been reported to range from 3.2%–5.5%.[3–5] Treatments for biliary complications include percutaneous abdominal drainage, percutaneous or endoscopic biliary drainage, balloon dilatation, and stent placement. However, if these therapies fail, one must consider surgical revision of the bile duct anastomosis. MCA developed by Yamanouchi et al[6,7] is a unique procedure to perform an alimentary tract anastomosis without surgical intervention. Recently, choledochocholedochostomy using MCA has been used for bile duct stenosis after dorsal pancreatectomy, major hepatectomy, and duct-to-duct biliary reconstruction in LDLT.[1,2] In the present case, conventional endoscopic therapy or a percutaneous transhepatic interventional radiological procedure failed to resolve the tough stricture of the bile duct after donor hepatectomy. MCA was attempted to avoid reoperation. The procedure was successful without adverse events.

REFERENCES

1. Itoi T, Kasuya K, Sofuni A, et al: Magnetic compression anastomosis for biliary obstruction: review and experience at Tokyo Medical University Hospital. J Hepatobiliary Pancreat Sci 18:357, 2011

2. Itoi T, Yamanouchi E, Ikeuchi N, et al: Magnetic compression duct-to duct anastomosis for biliary obstruction in a patient with living donor liver transplantation. Gut Liver 4:96, 2010

3. Taketomi A, Morita K, Toshima T, et al: Living donor hepatectomies with procedures to prevent biliary complications. J Am Coll Surg 211:456, 2010

4. Hwang S, Lee SG, Lee YJ, et al: Lessons learned from 1,000 living donor liver transplantations in a single center: how to make living donations safe. Liver Transpl 12:920, 2006

5. Kokudo N, Sugawara Y, Imamura H, et al: Tailoring the type of donor hepatectomy for adult living donor liver transplantation. Am J Transplant 5:1694, 2005

6. Yamanouchi E, Kawaguchi H, Endo I, et al: A new interventional method: magnetic compression anastomosis with rare-earth magnets. Cardiovasc Intervent Radiol 21:S155, 1998

7. Yamanouchi E, Kumano R, Kobayashi K, et al: Treatment for bowel or biliary obstruction by magnetic compression anastomosis development of Yamanouchi's method and its clinical evaluation (Japanese). J Nippon Med Sch 69:471, 2002

World Journal of Hepatology

Online Submissions: http://www.wjgnet.com/1948-5182office
wjh@wjgnet.com
doi:10.4254/wjh.v4.i4.139

World J Hepatol 2012 April 27; 4(4): 139-148
ISSN 1948-5182 (online)

ORIGINAL ARTICLE

Identification of cellular genes showing differential expression associated with hepatitis B virus infection

Yasuo Fukuhara, Takeshi Suda, Makoto Kobayashi, Yasushi Tamura, Masato Igarashi, Nobuo Waguri, Hirokazu Kawai, Yutaka Aoyagi

Yasuo Fukuhara, Takeshi Suda, Makoto Kobayashi, Yasushi Tamura, Masato Igarashi, Nobuo Waguri, Hirokazu Kawai, Yutaka Aoyagi, Division of Gastroenterology and Hepatology, Graduate School of Medical and Dental Sciences, Niigata University, 1-757 Asahimachi-dori, Chuo-ku, Niigata, Niigata 951-8122, Japan

Author contributions: Fukuhara Y and Suda T designed the research; Fukuhara Y, Kobayashi M, Tamura Y and Igarashi M performed the research; Waguri N and Kawai H contributed to data manipulation; Suda T and Aoyagi Y analyzed the data; and Takeshi Suda wrote the paper.

Correspondence to: Takeshi Suda, MD, Division of Gastroenterology and Hepatology, Graduate School of Medical and Dental Sciences, Niigata University, 1-757 Asahimachi, Niigata 951-8122, Japan. suda@med.niigata-u.ac.jp

Telephone: +81-25-227-2207 Fax: +81-25-227-0776

Received: March 25, 2011 Revised: September 6, 2011
Accepted: April 24, 2012
Published online: April 27, 2012

Abstract

AIM: To investigate the impact of hepatitis B virus (HBV) infection on cellular gene expression, by conducting both *in vitro* and *in vivo* studies.

METHODS: Knockdown of HBV was targeted by stable expression of short hairpin RNA (shRNA) in huH-1 cells. Cellular gene expression was compared using a human 30K cDNA microarray in the cells and quantified by real-time reverse transcription-polymerase chain reaction (RT-PCR) (qRT-PCR) in the cells, hepatocellular carcinoma (HCC) and surrounding non-cancerous liver tissues (SL).

RESULTS: The expressions of HBsAg and HBx protein were markedly suppressed in the cells and in HBx transgenic mouse liver, respectively, after introduction of shRNA. Of the 30K genes studied, 135 and 103 genes were identified as being down- and up-regulated, respectively, by at least twofold in the knockdown cells. Functional annotation revealed that 85 and 62 genes were classified into four up-regulated and five down-regulated functional categories, respectively. When gene expression levels were compared between HCC and SL, eight candidate genes that were confirmed to be up- or down-regulated in the knockdown cells by both microarray and qRT-PCR analyses were not expressed as expected from HBV reduction in HCC, but had similar expression patterns in HBV- and hepatitis C virus-associated cases. In contrast, among the eight genes, only *APM2* was constantly repressed in HBV non-associated tissues irrespective of HCC or SL.

CONCLUSION: The signature of cellular gene expression should provide new information regarding the pathophysiological mechanisms of persistent hepatitis and hepatocarcinogenesis that are associated with HBV infection.

Key words: Hepatitis B virus; Differential gene expression; Hepatocellular carcinoma; Gene expression signature; Adipose most abundant 2

Peer reviewers: Fei Chen, Associate Professor, Wayne State University, 259 Mack Avenue, Detroit, MI 48201, United States; George G Chen, Professor, Department of Surgery, The Chinese University of Hong Kong, Prince of Wales Hospital, CUHK, Shatin, NT, Hong Kong, China

Fukuhara Y, Suda T, Kobayashi M, Tamura Y, Igarashi M, Waguri N, Kawai H, Aoyagi Y. Identification of cellular genes showing differential expression associated with hepatitis B virus infection. *World J Hepatol* 2012; 4(4): 139-148 Available from: URL: http://www.wjgnet.com/1948-5182/full/v4/i4/139.htm DOI: http://dx.doi.org/10.4254/wjh.v4.i4.139

INTRODUCTION

Hepatitis B virus (HBV) is a major causative agent of chronic liver diseases that lead to the development of hepatocellular carcinoma (HCC) worldwide[1]. Vaccination against HBV has been proven efficacious for the prevention of virus transmission and has markedly reduced the carrier rate[2]. Several anti-viral agents, such as entecavir and interferon-α, also exert therapeutic effects by reducing virus titer[3]. Unfortunately, these preventative and therapeutic treatments are not widely administered, especially in areas with HBV epidemics[4]. Small molecule therapies and interferon treatments suffer from a number of drawbacks, including the selection of drug-resistant mutants, toxicity and limited efficacy[5,6]. Furthermore, the increase in international travel has introduced different genotypes of HBV to the world's populations, which may not be efficiently protected by the vaccine developed against the endemic genotype[7]. The World Health Organization reported that an estimated 350 million people worldwide are chronically infected with HBV and a significant proportion of chronic infections terminate in HCC, leading to more than half a million deaths annually (http://www.who.int/mediacentre/factsheets/fs204/en/). Thus, the need to elucidate the detailed pathophysiology of HBV infection is great.

Recent advancements in technology allow us to evaluate the proteome or transcriptome during pathogenic processes, providing new insight in terms of host-pathogen interactions. So far, *in vivo* cellular reactions associated with HBV infection have mainly been evaluated by comparing HBV-associated HCC [HCC(B)] with other liver tissues. Kim *et al*[8] reported a characteristic protein profile of HCC(B) in comparison with hepatitis C virus (HCV)-associated HCC [HCC(C)]. Differential gene expression profiles have also been reported in HCC(B) in comparison with corresponding surrounding liver tissues (SL)[9] or HCC(C)[10]. Although reduced tumorigenicity after knockdown of HBx protein has been reported in PLC/PRF/5 HCC cells[11], it is unclear whether HBV still has significant effects on cellular gene expression once the cells have been transformed because, at the time of HCC development, tumor cells no longer allow efficient viral expression[12,13]. In addition, it is reasonable to assume that malignant transformation causes a significant alteration of the gene expression signature and may overcome the impact of HBV on the profile. Thus, a simple HCC-oriented observation may not accurately reflect the cellular events induced by HBV infection.

Artificial control of HBV expression is another approach to studying differential cellular gene expression. Otsuka *et al*[14] reported that, in comparison with parental cells, several cellular genes were specifically up- or down-regulated in HepG2.2.15 cells, which are derived from HepG2 cells by transfecting them with plasmids containing HBV DNA, leading to the production of HBV proteins. Alteration of cellular gene expression has also been reported in HepG2.2.15 cells after knockdown of HBV through RNA interference (RNAi)[15]. Furthermore, microarray analysis has revealed differential cellular gene expression between wild-type and HBV transgenic mouse livers[16,17]. There are concerns, however, that the methodologies employed may have direct effects on cellular gene expression. There are inconsistencies in the genes that have been reported to be altered as a result of HBV infection, not only among studies using different models of HBV infection, but also using the same methodologies[18].

In this report, we elucidate the differentially expressed cellular genes associated with HBV infection by sequentially applying two processes: (1) selection of candidate genes by knockdown of HBV expression using RNAi in cells derived from a HBV-associated case; and (2) quantification of the selected gene expression in various liver tissues from both HBV-infected and non-infected patients. The advantage of our approach and the pathophysiological implications of our results are discussed.

MATERIALS AND METHODS

Design and construction of shRNA

Seventeen HBV genome sequences from GenBank were aligned and analyzed to identify the conserved regions containing at least nineteen contiguous nucleotides spanning within the region that was shared by all four open reading frames. Nineteen nucleotides following AA were common for all genotypes except for F and H, which are quite rare in Japan, and were further analyzed by BLAST to ensure that the sequence does not have significant homology with known human genes. Finally, the selected sequence, 5'-TGTCAACGACCGACCTTGA-3', was designed to form a hairpin structure when transcribed and cloned into pSUPER.retro (OligoEngine, WA, United States), which generates 3'-UU overhanging transcripts without a poly-A tail under the control of the polymerase-III H1-RNA gene promoter. Plasmids containing the target sequence or the same sequence with an A to G transition at the ninth nucleotide were designated pSUPER.HB4 or pSUPER.HB4G, respectively.

Cell culture and transfection

huH-1 cells; JCRB0199, were obtained from the JCRB cell repository and transfected with 2 μg of plasmids using Effectene transfection reagent (QIAGEN, Hilden, Germany) according to the manufacturer's instructions. In brief, 5.0×10^5 huH-1 cells were seeded into a 60 mm dish a day before transfection and the plasmids were mixed with 16 μL of enhancer followed by the addition of 50 μL Effectene reagents. After mixing with medium, the mixture was applied onto the culture plate. The stable transformants with pSUPER.retro, pSUPER.HB4 and pSUPER.HB4G were named huHpS, huHB4 and huHB4G, respectively.

Evaluation of HBsAg and HBx expression

The cells of 1×10^6/mL were subjected to culture and supernatants were collected on days 2 and 4 and stored at -20 ℃ until use. HBsAg was quantified in the medium by

a chemiluminescence immunoassay using ARCHITECT HBsAg QT (Abbott Japan Co. Ltd., Chiba, Japan).

Hydrodynamic gene delivery was employed[19] to target HBx in HBx transgenic mice[20] by injecting 100 μg of pSUPER.retro, pSUPER.HB4 or pSUPER.HB4G. Immunohistochemistry was performed on the liver specimens, which were obtained 48 hours after delivery, by a standard avidin-biotin complex method[21] that involved incubating the sections with primary antibodies of rabbit polyclonal anti-HBx[22].

cDNA microarray analysis

Total RNA was isolated from huHpS and huHB4 cells using IsoGen (Nippon Gene Co. Ltd., Tokyo, Japan) and stored at -80 ℃. After amplification by T7 polymerase, cDNAs were labeled with the fluorescent dyes cy3 or cy5, and hybridized with AceGene human 30K cDNA microarrays (DNA Chip Research Inc. Yokohama, Japan), which contain 32 000 sequences verified by the mouse IMAGE consortium (http://image.hudsonalpha.org/). After washing, the arrays were scanned and the signal intensity of a spot was considered significant if the intensity was 200 times greater than the background; otherwise, the spot was flagged as "not found". Using TIGR MIDAS software (http://www.tm4.org/), the data obtained from qualified spots were normalized by applying the LOWESS algorithm. After normalization, the spots were judged to be inconsistent between a pair of flip-dye replicates and filtered out, if $\log_2(cy3/cy5)/\log_2(cy5/cy3)$ was outside the range from -1 to 1. We took a difference of spot intensities between huHB4 and huHpS of more than double or less than half as significant. The selected genes were fed to the DAVID functional annotation tool (http://david.abcc.ncifcrf.gov/home.jsp).

Quantitative real-time reverse transcription-polymerase chain reaction

Total RNAs of huH-1 cells and liver tissues were purified with RNeasy Mini kits (QIAGEN KK, Tokyo, Japan) after digestion with RNase-free DNase I (Invitrogen Corporation, Carlsbad, United States) and were reverse transcribed for use in TaqMan Gene Expression Assays using a LightCycler (Roche Diagnostics, Mannheim, Germany). To quantify the expression of the candidate genes selected in microarray analyses and of the internal controls, hypoxanthine phosphoribosyltransferase 1 (*HPRT1*) and beta 2-microglobulin (*β2M*), commercially available primer and probe sets were employed, whereas custom primers, 5'-CCCGTCTGTGCCTTCTCA-3' and 5'-GGTCGGTCGTTGACATTGCT-3', and a probe, 5'-CCGTGTGCACTTCGCT-3', sequences that are common to all four open reading frames, were designed by Custom TaqMan® Gene Expression Assay (Applied Biosystems Inc., Foster City, United States) for HBV expression. The results were analyzed using LightCycler software (Roche Diagnostics, Mannheim, Germany). A relative fluorescent intensity was calculated from a standard curve obtained by quantitative analyses using a serial dilution of total RNA from HepG2. Finally, a relative amount of each message was calculated as a ratio of threshold cycle after normalization against *HPRT1* or *β2M*.

Liver tissue samples

Liver tissue samples were obtained from surgical resections of HCC or other cancers from eighteen patients consisting of five HBV-positive cases, five HCV-positive cases, three neither HBV nor HCV positive cases, and five cases without chronic liver disease, which included one colon cancer, one common bile duct cancer and three rectal cancer cases. The three patients without viral hepatitis had autoimmune hepatitis, primary biliary cirrhosis and alcoholic liver cirrhosis. No cases showed positive reactions to HBsAg or anti-HBc, except for the HBV-positive cases. Two expert pathologists independently evaluated liver specimens. Each HBV-positive or HCV-positive group consisted of two chronic hepatitis cases and three cirrhotic cases. Written informed consent was obtained from each patient and the study protocol conformed to the ethical guidelines of the 2008 Declaration of Helsinki, as reflected in prior approval by the Niigata University Graduate School of Medical and Dental Sciences Human Research Committee.

Statistical analysis

Doubling times of the cells and quantity of HBsAg in cultured medium were compared using ANOVA analysis followed by post hoc Bonferroni's multiple comparison tests, whereas the Mann-Whitney test was employed to compare HBV expression between HCC(B) and SL(B). In the DAVID annotation system, Fisher's exact test was adopted to measure the gene enrichment in annotation terms by referencing the frequencies of 30 000 genes of the human genome. All analyses except for the functional annotation were performed using GraphPad Prism 5 (GraphPad Software, Inc. La Jolla, United States) and a two-sided P value less than 0.05 was considered statistically significant.

RESULTS

Stable expression of shRNA is effective for knockdown of various HBV transcripts

We cloned huHB4G and huHB4, in which shRNA for the HBx coding region is continuously expressed in huH-1 cells with and without nucleotide replacement at the center from A to G, respectively. The cells transfected with plasmids with no insert were referred to as huHpS.

Morphologically, no remarkable differences were observed among the clones in culture, as shown in Figure 1A. The average doubling times in three independent cultures of huHpS, huHB4G and huHB4 were 40.9 ± 1.8 h, 46.8 ± 2.6 h and 45.1 ± 1.2 h, respectively, and were not significantly different between huHpS and huHB4, but were different between huHpS and huHB4G (P = 0.022). To evaluate the efficacy of the shRNA, HBsAg was quantified in the culture medium. Its concentrations

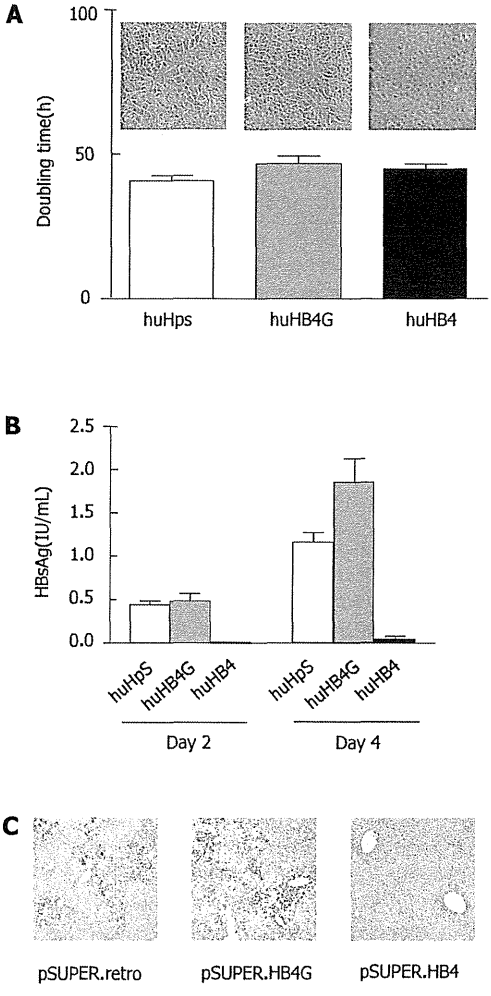

Figure 1 Effects of short hairpin RNA targeting hepatitis B virus on huH-1 cells. A sequence of nineteen nucleotides that is shared by all four open reading frames of HBV was cloned into pSUPER.retro and named pSUPER. HB4, which was further mutated at the ninth A to G and designated pSUPER. HB4G. Stable transformants of each plasmid in huH-1 cells were established as huHpS, huHB4 and huHB4G, respectively. A: Representative morphologies (upper panel) and average doubling times (lower graph) of each transformant. Each stable transformant was maintained at 37 °C with 5% CO_2 in Dulbecco's modified Eagle's medium supplemented with 10% fetal bovine serum and microscopically observed after 48 h (original magnification: 10x). The cells were counted on days 2 and 4 to calculate the average doubling times of each cell line from three independent cultures (40.9 ± 1.8 h, 46.8 ± 2.6 h and 45.1 ± 1.2 h in huHpS, huHB4G, and huHB4, respectively). The observed doubling times were not significantly different between huHpS and huHB4 but were different between huHpS and huHB4G (P = 0.022); B: The concentrations of HBsAg in the culture medium from huHpS, huHB4G, and huHB4 were 0.44 ± 0.046 IU/mL, 0.48 ± 0.091 IU/mL and 0.010 ± 0.0016 IU/mL on day 2 and 1.16 ± 0.11, 1.86 ± 0.26, and 0.050 ± 0.036 IU/mL on day 4, respectively. On both days, HBsAg was significantly reduced in huHB4 compared with the other two clones, but it was increased in huHB4G compared with huHpS (P = 0.0001 and P < 0.0001, respectively). C: Immunohistochemistry for HBx protein in HBx transgenic mouse liver 48 h after hydrodynamic gene delivery of pSUPER.retro, pSUPER.HB4G or pSUPER.HB4. The positive signals were remarkably reduced in mice that received pSUPER.HB4 compared with mice that received the other vectors, but were rather overrepresented in pSUPER.HB4G compared with pSUPER.retro (original magnification: 4x).

were 0.44 ± 0.046 IU/mL, 0.48 ± 0.091 IU/mL and 0.010 ± 0.0016 IU/mL on the second day and 1.16 ± 0.11 IU/mL 1.86 ± 0.26 IU/mL and 0.050 ± 0.036 IU/mL on the fourth day, respectively (Figure 1B). On both days 2 and 4, HBsAg was significantly reduced in huHB4 compared with the other two clones, but was increased in huHB4G compared to huHpS (P = 0.0001 and P < 0.0001, respectively).

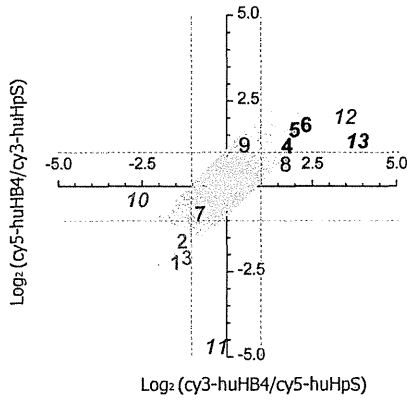

Figure 2 Log2 plot of flip-dye conversion in microarray analysis between huHpS and huHB4. Total RNAs from huHpS and huHB4 were labeled with cy3/cy5, or vice versa, and subjected to a human 30 K cDNA microarray. Log2 ratios of the intensities in each labeling combination were plotted after LOWESS normalization as long as signal intensities were consistent between dye-flipping with less than a twofold difference. In total, 13 012 spots were plotted, and the dotted lines indicate a log2 intensity ratio of 1 or -1. Numbers 1 to 13 indicate the spots that were randomly selected for further quantitative reverse transcription-polymerase chain reaction evaluation. Bold gray and black numbers represent the spots that were found to show a twofold higher or lower intensity in huHB4 compared with huHpS by both microarray and quantitative RT-PCR analyses. Italicized numbers indicate the flip-inconsistent spots. RT-PCR: Real-time reverse transcription-polymerase chain reaction.

Next, the plasmids were delivered to hepatocytes in HBx transgenic mice using hydrodynamic gene delivery. After 48 h, the mouse livers were harvested and an immunohistochemical analysis was performed for HBx protein. As shown in Figure 1C, the positive signals were remarkably reduced in mice that received pSUPER.HB4 compared with other mice and were rather overrepresented in pSUPER.HB4G compared to pSUPER.retro.

Cellular gene expression was affected by knockdown of HBV messages

Because pSUPER.HB4G is suggested to have the potential enhancing HBV expression, gene expression signatures were compared between huHB4 and huHpS using a human cDNA microarray. Of 29 953 effective spots, LOWESS normalization validated 19 923 and 20 926 signals in each dye-sample combination, leading to final validation of 18 288 spots for both dye combinations. Additionally, 5276 signals were eliminated based on a flip-dye inconsistency greater than twofold, resulting in 13 012 genes available for further evaluation (Figure 2). Among those, 145 and 103 genes were down- and up-regulated, respectively, by at least twofold in huHB4 cells compared to huHpS cells (Supplementary Table 1, Supplementary material online). In order to exclude genes

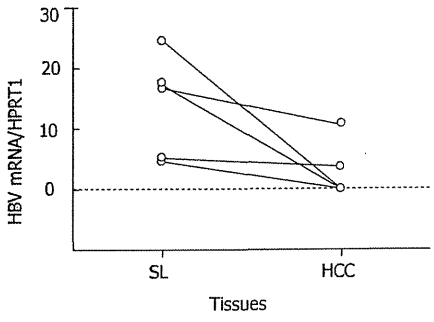

Figure 3 Quantity of hepatitis B virus mRNA in hepatocellular carcinoma and surrounding liver tissues. The total amount of hepatitis B virus (HBV) mRNA was quantified as a ratio relative to hypoxanthine phosphoribosyltransferase 1 message in hepatocellular carcinoma (HCC) and surrounding noncancerous liver tissues (SL) from five HBV-associated cases. In all cases, the message was repressed in HCC, and the average was significantly reduced from 13.7 ± 8.6 to 2.9 ± 4.7 (P = 0.032).

that might be repressed by off-targeting effects, the 13 012 genes were evaluated using a siRNA seed locator (http://www.dharmacon.com/seedlocator/default.aspx). A total of 1063 genes were found to have at least one match with our shRNA target sequence and ten genes were included in the 145 repressed genes. Thus, 135 repressed and 103 enhanced genes were selected as final candidates.

To confirm the microarray results, thirteen genes were randomly selected from the first and third quadrants of the $\log_2$(cy3-huHB4/cy5-huHpS)-$\log_2$(cy5-huHB4/cy3-huHpS) plot for the 18 288 LOWESS-validated genes and subjected to quantified by real-time reverse transcription-polymerase chain reaction (qRT-PCR) (Table 1). Of the thirteen genes, nine genes were chosen from the 13 012 flip-consistent genes, whereas the other four genes were selected from the 5276 flip-inconsistent genes. The flip-consistent genes were further divided into three groups of three genes each according to their intensity ratio of huHB4/huHpS: (1) less than 0.5 in both dye combinations; (2) more than 2 in both dye combinations; or (3) between 0.5 and 2 in at least one combination. In all flip-consistent genes, the relative quantities were not remarkably different between the two references of *HPRT1* and *β2M*, and gene expression patterns were quite similar between microarray and qRT-PCR analyses. On the other hand, the four flip-inconsistent genes showed various expression patterns in qRT-PCR analysis. Two genes were found to express less or more than twofold in huHB4, whereas the expression differences were approximately twofold for the other two genes. These results suggest that the final 238 candidate genes are highly likely to have altered gene expression of a more than twofold magnitude in both microarray and qRT-PCR analyses.

To mine functional annotation, a list of the candidate genes was uploaded to DAVID program. Of 238 genes, 62 up- and 85 down-regulated genes were annotated and identified as being enriched into four and five representative functional categories, respectively, based on the controlled vocabulary of the Gene Ontology Consortium, as shown in Table 2. The up-regulated genes were classified

Table 1 Microarray and quantitative reverse transcription-polymerase chain reaction for candidate genes

No.	Genes	Microarray[3]		qRT-PCR[4]		Accession number[5]
		cy3/cy5	cy5/cy3	/β2M	/HPRT1	
1	*CSTA*[1]	0.35	0.26	0.23	0.23	NM_005213
2	*APM2*[1]	0.46	0.31	0.22	0.23	NM_006829
3	*SLPI*[1]	0.47	0.31	0.08	0.09	NM_003064
4	*CTGF*[1]	3.36	2.026	3.49	3.93	NM_001901
5	*NADE*[1]	3.89	2.85	3.99	4.48	AF187064
6	*TTR*[1]	5.13	3.07	4.6	5.3	NM_000371
7	*ARL3*	0.59	0.52	0.54	0.62	NM_004311
8	*GCNT3*	3.2	1.97	1.74	1.95	NM_004751
9	*NRF-1*	1.42	2.16	0.98	1.12	L22454
10	*KIAA1808*[1,2]	0.16	0.85	0.34	0.4	AB058711
11	*HSPC159*[2]	0.9	0.04	0.66	0.77	NM_014181
12	*MAP2K6*[2]	11.08	3.76	1.68	1.89	NM_002758
13	*SKAP2*[1,2]	13.45	2.33	2.03	2.34	NM_003930

[1]huHpS > 2x huHB4 or 2x huHpS < huHB4, respectively, in both microarray and qRT-PCR; [2]flip-inconsistent spots; [3]a signal intensity ratio of huHB4/huHpS; [4]relative expression in huHB4 against in huHpS normalized by beta 2-microglobin (*β2M*) or hypoxanthine phosphoribosyl transferase 1 (*HPRT1*); [5]GenBank accession number. qRT-PCR: Quantified by real-time reverse transcription-polymerase chain reaction.

into groups of lipid synthesis, glycoprotein, biopolymer metabolism and hydrolase activity. Genes that function as signal peptides, protease inhibitors and cytokines and in sensory perception and transport were significantly enriched in the down-regulated genes.

Evaluation of candidate gene expression in livers with various disorders

The differential expression in microarray analysis was validated by qRT-PCR using HCC and SL tissues from eighteen livers. Expression levels of the eight genes, which are listed as genes 1 to 6, 10 and 13 in Table 1, were quantified. Four genes were suppressed and the other four genes were enhanced more than twofold in huHB4. In HBV-associated tissues, HBV expression was also quantified. As shown in Figure 3, the average relative HBV expressions were 2.9 ± 4.7 and 13.7 ± 8.6 in HCC(B) and SL(B), respectively, and were a significantly decreased in HCC(B) (P = 0.032).

As shown in Figure 4A, all $\log_2$ ratios of SL(C), SL(NBNC) and SL(N) to SL(B) were distributed between -1 and 1, except for *CSTA*, *APM2*, *CTGF* and *TTR*, which showed expressions in SL(B) at magnitudes of 7.7-, 2.5-, 2.6- and 2.3-fold in comparison with SL(C), SL(C), SL(N) and SL(C), respectively. The reduced expression patterns in liver tissues without HBV infection are consistent with the results in huHB4 only for *CSTA* and *APM2*. In comparisons of HCC(C) and HCC(NBNC) with HCC(B), several genes showed expression differences of more than twofold that were consistent with differential expression in huHB4 (Figure 4B). Of the four genes that had low expression in huHB4, *APM2* also had low expression in both HCC(C) and HCC(NBNC), with magnitudes of 0.074 and 0.11, respectively. *SLPI* and

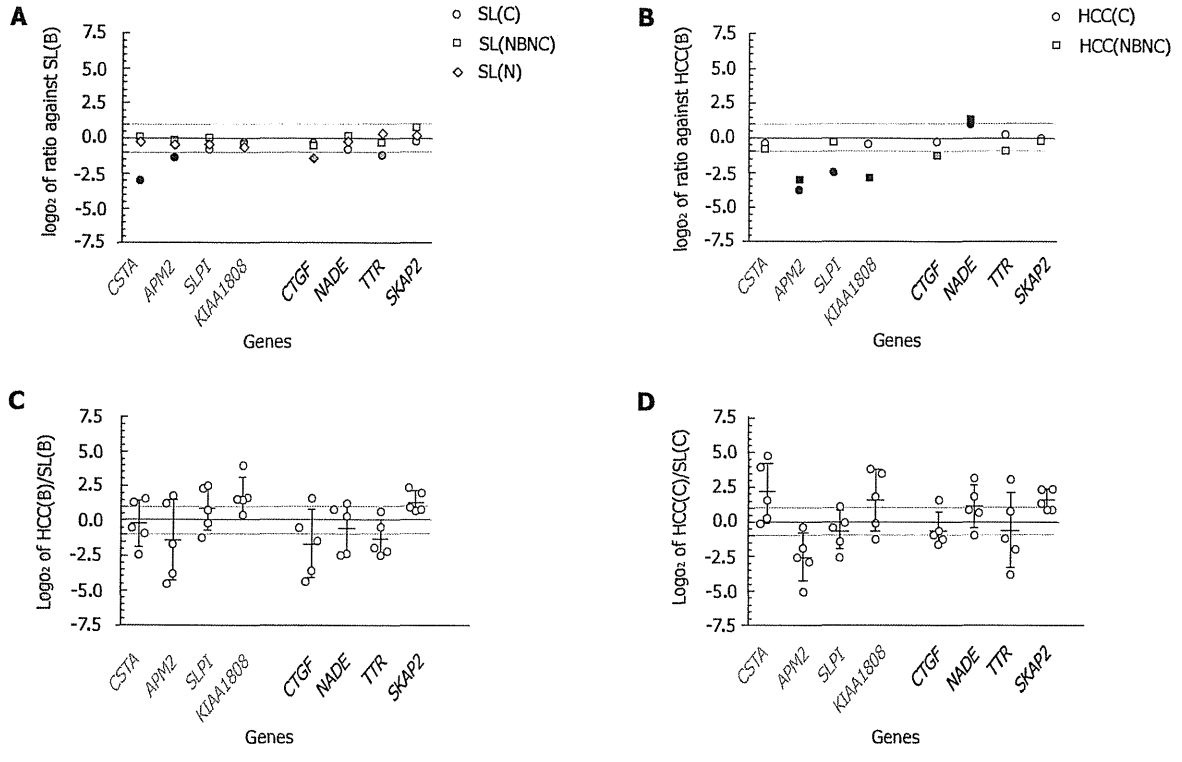

Figure 4 Expression profiles in various liver tissues with respect to genes differentially expressed in huHB4. Quantitative RT-PCR was performed using various liver tissues for eight genes that were confirmed to be differentially expressed with HBV knockdown in huH-1 cells by both microarray and quantitative RT-PCR. The genes included *CSTA*, *APM2*, *SLPI* and *KIA1808*, which are down-regulated, and *CTGF*, *NADE*, *TTR* and *SKAP2*, which are up-regulated in huHB4 knockdown cells. Relative amounts of each message are plotted as log2 ratios, and the dotted gray lines indicate 1 and -1 log2 ratios. Liver tissues include five HBV infected cases (B), five HCV infected cases (C), three neither HBV nor HCV infected cases (NBNC) and five cases without chronic liver diseases (N). A: Comparison between surrounding non-cancerous liver tissues (SL). The combinations include comparisons of SL(B) to SL(C), SL(NBNC) and SL(N); B: Comparisons between HCC. The combinations include comparisons of HCC(B) to HCC(C) and to HCC(NBNC). In A and B, the results are plotted in white if the ratio was between 1 and -1, whereas black and gray marks indicate consistency and inconsistency between the results from liver tissues and huHB4, respectively. C, D: Log2 ratio between HCC(B) and the corresponding SL(B), or HCC(C) and corresponding SL(C). The error bars indicate mean ± SD. RT-PCR: Real-time reverse transcription-polymerase chain reaction; HBV: Hepatitis B virus; HCV: Hepatitis C virus; HCC: Hepatocellular carcinoma; SL: Surrounding non-cancerous liver tissues.

KIAA1808 expression were also decreased in HCC(C) and HCC(NBNC) to 0.17- and 0.13-fold, respectively. On the other hand, only NADE exhibited differential expression larger than twofold, a pattern consistent with that seen in huHB4, and it was expressed 2.0- and 2.4-fold higher in HCC(C) and HCC(NBNC), respectively.

On the other hand, the comparison of gene expression between HCC and SL from the same individual suffering from HBV infection showed wide variation among cases (Figure 4C). Only *SKAP2* exhibited more than a twofold difference with relatively smaller variation and was expressed at 2.60 ± 1.07-fold higher in HCC(B). None of the eight candidates showed expression differences of more than twofold in all the five cases examined. Wide variation was also observed in HCV-associated cases, with a pattern similar to that seen in HBV-associated cases, as represented by *SKAP2* (Figure 4D).

DISCUSSION

Consistent with previous reports[12,13], we found that HBV expression was significantly reduced in HCC(B) compared to the corresponding SL(B) in all of our cases. In order to mimic physiological repression of HBV expression through hepatocarcinogenesis, a sustained induction of RNAi against HBV was employed in this study. A single target of shRNA for a shared sequence in all four transcripts from HBV successfully achieved substantial reduction of HBsAg and HBx protein expressions *in vitro* and *in vivo*, respectively, without affecting cell morphology or replication rate.

RNAi is an evolutionarily conserved mechanism of post-transcriptional gene silencing induced by dsRNA and has been widely studied to prove its efficacy in reverse functional genomics and for therapeutic use[23,24]. Unfortunately, it is important to remember that the modulation of gene expression through RNAi can be extended to unintended genes due to various processes including off-target effects[25]. Off-target effects, which are RNAi-mediated events affecting the expression levels of dozens to hundreds of genes, are quite difficult to completely eliminate because off-targeting can be mediated by complementarity even between a hexamer seed region of dsRNA and the 3' untranslated region of a target[26]. It has been reported that using different siRNA sequences that target HBV in HepG2.2.15 cells leads to different cellular gene expression profiles, suggesting a complicated influence of siRNA on cellular gene expression[18].

Table 2 Representative genes in enriched functional categories

Category	No. of genes	*P* value[1]	Genes	Accession number[2]
Up regulated				
Lipid synthesis	3	0.01	*3-hydroxy-3-methylglutaryl-coenzyme A reductase*	NM_000859
			7-dehydrocholesterol reductase	NM_001360
			Growth differentiation factor 1	M62302
Glycoprotein	15	0.019	*Integrin beta 3*	NM_000212
			Interleukin 1 alpha	NM_000575
			Vitronectin	NM_000638
Biopolymer metabolism	16	0.02	*Cell division cycle 7*	NM_003503
			Colony stimulating factor 1 receptor	NM_005211
			Connective tissue growth factor	NM_001901
Hydrolase activity	6	0.046	*Bile acid coenzyme A: amino acid n-acyltransferase*	NM_001701
			Inositol polyphosphate-5-phosphatase	AF184215
			Poly(A)-specific ribonuclease	AJ005698
Down regulated				
Signal	17	0.001	*Cytotoxic T-lymphocyte-associated protein 4*	NM_005214
			Epithelial cell adhesion molecule	NM_002354
			Gamma-aminobutyric acid A receptor alpha 4	NM_000809
Protease Inhibitor	3	0.024	*Cystatin A*	BC010379
			Secretory leukocyte peptidase inhibitor	NM_003064
			Tissue factor pathway inhibitor	AF021834
Sensory perception	3	0.024	*Collagen type I alpha 2*	NM_000089
			GATA binding protein 3	BC006839
			USHER syndrome 1C	NM_005709
Transport	7	0.031	*Amyloid beta precursor protein binding family A member 2*	BC007794
			ATP-binding cassette subfamily D member 4	NM_020323
			Solute carrier family 17 member 2	AL138726
Cytokine activity	4	0.046	*Chemokine ligand 25*	AB046579
			Kit ligand	NM_000899
			Prolactin	NM_000948

[1]Probability of gene enrichment calculated using Fisher's exact test by referencing the frequency in 30 000 genes of human genome background; [2]GenBank accession number.

In this study, a seed locator program found at least one match in approximately 8% of 13 012 genes, even after the target sequence was carefully selected to make sure that no known cellular gene would show homology in its coding sequence with the target. Furthermore, pSUPER. HB4G unexpectedly up-regulated the expression of both HBsAg and HBx. It seems prudent to assume that cellular genes selected by knockdown experiments using RNAi against HBV involve genes directly affected by the RNAi process. In this regard, it is quite important to validate the results from *in vitro* experiments in liver tissues.

When human liver tissues were evaluated to find genes that are involved in hepatocarcinogenesis under HBV infection, gene expression profiles were generally compared between HCC(B) and SL(B). It is thought, however, that the transformation process itself requires a tremendous alteration of cellular gene expression, irrespective of etiology, that may outstrip the impact of HBV infection on the cellular gene expression. This concern seems to be relevant because qRT-PCR using liver tissues revealed that the differential expression patterns between HCC(B) and SL(B) were inconsistent with those between huHB4 and huHpS, but quite resembled the patterns between HCC(C) and SL(C). It would be ideal to evaluate the effect of HBV on cellular gene expression using non-tumorous liver tissues from the same individual at various time points with different levels of HBV expression, such as before and after natural seroconversion. In reality, however, it is quite difficult to collect liver specimens repeatedly in those settings.

To address this issue, HBV-associated liver tissues were compared with various liver tissues from the same individual and others. The major factors considered in comparisons among patients should be (1) with or without chronic liver diseases; (2) viral or non-viral liver diseases; and (3) cancerous or non-cancerous liver tissues. Thus, in the present study, gene expression levels in HCC(B) and SL(B) were compared with those in HCC(C), HCC(NBNC), SL(C), SL(NBNC) or SL(N). Because the presence or absence of viral infection presumably has a substantial impact on the cellular gene expression profile irrespective of virus species, the comparison between SL(B) and SL(NBNC) or between SL(B) and SL(N) does not reflect the specific influence of HBV infection, but of viral hepatitis in general. The cellular genes that are strictly regulated in connection with HBV infection should be differentially expressed, not only between HCC(B) and HCC(C), but also between SL(B) and SL(C). Among eight candidates, only *APM2* fulfilled those criteria in this study. Thus, *APM2*, which is confirmed to be repressed after reduction of HBV expression in both RNAi knockdown experiments and liver tissues, is highly likely to be differentially expressed in association with HBV infection.

APM2 is a gene located on chromosome 10 at q23.2 and was originally identified as the second most abundant transcript in adipose tissue following adiponectin, *APM1*[27]. It is reported, however, that *APM2* is expressed in a wide variety of tissues, including the liver[28], and is dysregulated in various cancers. Up-regulation of *APM2* has been reported in pancreatic intraepithelial neoplasms[29], breast cancer tissues from patients with poor prognoses[30], and cisplatin-resistant gastric cancer cell lines[31]. Furthermore, overexpression of *APM2* is reported to promote cisplatin resistance in a variety of cancer cell types[32]. Although the exact function of *APM2* is currently unknown, these observations suggest that *APM2* plays a role as an anti-apoptotic factor. HBV infection may induce sustained expression of *APM2*, leading to persistent viral infection and hepatocarcinogenesis. It would be interesting to determine whether HCC(B) is more resistant to cisplatin than HCC(C) and/or HCC(NBNC) because *APM2* expression is substantially higher in HCC(B).

In the present study, 32 000 initial genes were evaluated, and of these genes, only one gene, *APM2*, was selected as a highly possible candidate gene that is differentially expressed due to HBV infection. Although we have so far evaluated only eight genes of 238 microarray candidates using human tissues, the concordance between the results from the cell lines and liver tissues is insufficient. It is true that the results obtained from the cell lines under shRNA overexpression technically involve many artificial limitations. However, another possible explanation for the low concordance is that cellular gene expression is regulated as a functional unit rather than by each gene. Functional annotations of genes selected in this study through microarray analysis indicated that the reduction of HBV expression led to disproportionately higher rates of increases or decreases of cellular gene expression in certain functional categories. The categories of genes with significantly enhanced or repressed expression after knockdown of HBV included lipid synthesis and protease inhibitors, respectively. In terms of lipid synthesis, for example, it has been reported that there is an inverse correlation between HBV and apolipoprotein expressions[33], and it is the largest functional category of lipid biosynthetic pathways to show differential expression between HBV transgenic and wild-type control mice[17]. Consistently, differential expression of cellular proteins were investigated in association with HBV infection and indicated that lots of proteins were up or down regulated as groups of several functional categories, including metabolisms[34-37]. Unfortunately, however, few reports applied the technologies of proteome or transcriptome analyses to human liver tissues instead of HBV-associated cell lines. To clarify the clinical significance of functional annotation, it is necessary to conduct proteome or transcriptome analyses on a large scale using liver tissues in various conditions.

In conclusion, it is suspected that the comparison between HCC(B) and SL(B) is not ideal for determining which genes are differentially expressed as a result of HBV infection. Because chronic viral hepatitis should have significant impacts on cellular gene expression, just as cellular transformation does, differential expression should be confirmed by comparing HBV-associated cases with HCV- or other viral-associated cases in terms of both HCC and SL. In the present study, the *APM2* gene was selected from 32 000 human genes as the gene that was differentially expressed in those settings. In the future, differential cellular gene expression should be evaluated with respect to functional categories based on proteome and/or transcriptome analyses. The knowledge of cellular gene expression will help to elucidate the detailed mechanisms involved in chronic hepatitis B and HBV-associated hepatocarcinogenesis.

SUPPLEMENTARY MATERIAL

Supplementary Table 1 is available at Supplementary material online (http://www.wjgnet.com/1948-5182/g_info_20120428090827.htm).

COMMENTS

Background

Powerful preventive and therapeutic means have been developed for hepatitis B virus (HBV) infection, such as vaccination and nucleotide analogue, on the basis of our knowledge for HBV life cycle. Unfortunately, however, the World Health Organization reported that an estimated 350 million people worldwide are chronically infected with HBV and a significant proportion of chronic infections terminate in hepatocellular carcinoma (HCC), leading to more than half a million deaths annually. These dreadful situations request thorough understanding of the mechanisms for HBV to persuade sustained infection and hepatocarcinogenesis.

Research frontiers

A recent technological advancement makes it possible to analyze an impact of a specific molecule such as HBV on the proteome and/or transcriptome in host cells. It is not difficult to assume that a deviation of gene expression profile plays a crucial role for immunological escape and cancer progression in HBV infection. The knowledge of HBV-host cell interaction must provide a powerful tool to fight HBV infection.

Related publications

So far, an alteration of gene expression profile due to HBV infection has mainly been evaluated between non-infected parental cells and artificially-infected cells or between cells that were established from HBV positive case and HBV-knockdown cells. In terms of clinical materials, the comparisons between HBV-associated HCC and corresponding noncancerous liver tissues or between HBV-positive and HBV-negative cancer cells have been reported.

Innovations and breakthroughs

In the knockdown or artificial infection of HBV, it is quite difficult to completely eliminate the impact of knockdown/infection treatment itself on cellular gene

expression. Furthermore, it is not difficult to assume that a malignant transformation process induces a tremendous change in cellular gene expression profile, which may overtake the effects of host-pathogen interactions. In order to avoid these confounding factors, the research team led by Takeshi Suda from Division of Gastroenterology and Hepatology, Niigata University took a two-step approach. Firstly, pick up candidate genes in a HBV-positive cell line by knocking HBV expression down, using small hairpin RNA, then confirm differential expression of the candidates in various liver tissues, including both cancer and noncancer associated with HBV, hepatitis C virus (HCV) or no HBV/HCV. Through this approach, the authors finally selected one gene, which differentially expressed in association with HBV infection, regardless of cancerous or noncancerous tissues.

Applications

The new insight of cellular reaction evoked by HBV infection must provide a clue to better understanding the mechanisms of sustained viral infection and cancer development, and will be implicated in the development of novel therapeutic options.

Terminology

RNA interference is a process within living cells, in which double-stranded RNA directs a gene activity control with certain sequence specificity. shRNA is a small hairpin RNA, and short hairpin RNA is a sequence of RNA that makes a tight hairpin turn that can induce RNA interference. Off-targeting is a phenomenon where genes with incomplete complementarities with a target sequence are regulated in RNA interference. Dye flip is a strategy to account for dye bias in microarray experiments by labeling of DNA targets with the two dyes in reciprocal fashion. APM2 was discovered as the second most abundant transcript in adipose tissue following adiponectin and has been reported to be expressed in a variety of other tissues, including liver. *APM2* gene overexpression is associated with malignant transformation and resistant to a chemotherapeutic agent have been reported.

Peer review

The authors provided evidence indicating that silencing HBV mRNA altered cellular gene expressions in several functional categories including lipid synthesis. By stably targeting the common ORF region of the key HBV protein genes with shRNA, they observed a substantial decrease of HBsAg expression and up- or down-regulation of cellular genes, as revealed by DNA microarray. To verify *in vitro* assay results, they extended the observations to human liver tissues. The conclusions provide new insights into the mechanisms of HBV- or HCV-induced chronic liver diseases and hepatocarcinogenesis, and would be very useful for identification of novel drug targets against HBV infection.

REFERENCES

1 **Shariff MI**, Cox IJ, Gomaa AI, Khan SA, Gedroyc W, Taylor-Robinson SD. Hepatocellular carcinoma: current trends in worldwide epidemiology, risk factors, diagnosis and therapeutics. *Expert Rev Gastroenterol Hepatol* 2009; **3**: 353-367

2 **Daniels D**, Grytdal S, Wasley A. Surveillance for acute viral hepatitis - United States, 2007. *MMWR Surveill Summ* 2009; **58**: 1-27

3 **Papatheodoridis GV**, Manolakopoulos S, Dusheiko G, Archimandritis AJ. Therapeutic strategies in the management of patients with chronic hepatitis B virus infection. *Lancet Infect Dis* 2008; **8**: 167-178

4 **Zanetti AR**, Van Damme P, Shouval D. The global impact of vaccination against hepatitis B: a historical overview. *Vaccine* 2008; **26**: 6266-6273

5 **Fontana RJ**. Side effects of long-term oral antiviral therapy for hepatitis B. *Hepatology* 2009; **49**: S185-S195

6 **Dienstag JL**. Benefits and risks of nucleoside analog therapy for hepatitis B. *Hepatology* 2009; **49**: S112-S121

7 **Tacke F**, Amini-Bavil-Olyaee S, Heim A, Luedde T, Manns MP, Trautwein C. Acute hepatitis B virus infection by genotype F despite successful vaccination in an immune-competent German patient. *J Clin Virol* 2007; **38**: 353-357

8 **Kim W**, Oe Lim S, Kim JS, Ryu YH, Byeon JY, Kim HJ, Kim YI, Heo JS, Park YM, Jung G. Comparison of proteome between hepatitis B virus- and hepatitis C virus-associated hepatocellular carcinoma. *Clin Cancer Res* 2003; **9**: 5493-5500

9 **Kim MY**, Park E, Park JH, Park DH, Moon WS, Cho BH, Shin HS, Kim DG. Expression profile of nine novel genes differentially expressed in hepatitis B virus-associated hepatocellular carcinomas. *Oncogene* 2001; **20**: 4568-4575

10 **Iizuka N**, Oka M, Yamada-Okabe H, Mori N, Tamesa T, Okada T, Takemoto N, Hashimoto K, Tangoku A, Hamada K, Nakayama H, Miyamoto T, Uchimura S, Hamamoto Y. Differential gene expression in distinct virologic types of hepatocellular carcinoma: association with liver cirrhosis. *Oncogene* 2003; **22**: 3007-3014

11 **Chan DW**, Ng IO. Knock-down of hepatitis B virus X protein reduces the tumorigenicity of hepatocellular carcinoma cells. *J Pathol* 2006; **208**: 372-380

12 **Raimondo G**, Burk RD, Lieberman HM, Muschel J, Hadziyannis SJ, Will H, Kew MC, Dusheiko GM, Shafritz DA. Interrupted replication of hepatitis B virus in liver tissue of HBsAg carriers with hepatocellular carcinoma. Virology 1988; 166: 103-112.

13 **Wang Y**, Wu MC, Sham JS, Tai LS, Fang Y, Wu WQ, Xie D, Guan XY. Different expression of hepatitis B surface antigen between hepatocellular carcinoma and its surrounding liver tissue, studied using a tissue microarray. *J Pathol* 2002; **197**: 610-616

14 **Otsuka M**, Aizaki H, Kato N, Suzuki T, Miyamura T, Omata M, Seki N. Differential cellular gene expression induced by hepatitis B and C viruses. *Biochem Biophys Res Commun* 2003; **300**: 443-447

15 **Giladi H**, Ketzinel-Gilad M, Rivkin L, Felig Y, Nussbaum O, Galun E. Small interfering RNA inhibits hepatitis B virus replication in mice. Mol Ther 2003; 8: 769-776

16 **Hu Z**, Zhang Z, Kim JW, Huang Y, Liang TJ. Altered proteolysis and global gene expression in hepatitis B virus X transgenic mouse liver. *J Virol* 2006; **80**: 1405-1413

17 **Hajjou M**, Norel R, Carver R, Marion P, Cullen J, Rogler LE, Rogler CE. cDNA microarray analysis of HBV transgenic mouse liver identifies genes in lipid biosynthetic and growth control pathways affected by HBV. *J Med Virol* 2005; **77**: 57-65

18 **Guo Y**, Guo H, Zhang L, Xie H, Zhao X, Wang F, Li Z, Wang Y, Ma S, Tao J, Wang W, Zhou Y, Yang W, Cheng J. Genomic analysis of anti-hepatitis B virus (HBV) activity by small interfering RNA and lamivudine in stable HBV-producing cells. *J Virol* 2005; **79**: 14392-14403

19 **Suda T**, Gao X, Stolz DB, Liu D. Structural impact of hydrodynamic injection on mouse liver. *Gene Ther* 2007; **14**: 129-137

20 **Kim CM**, Koike K, Saito I, Miyamura T, Jay G. HBx gene of hepatitis B virus induces liver cancer in transgenic mice. *Nature* 1991; **351**: 317-320

21 **Igarashi M**, Suda T, Hara H, Takimoto M, Nomoto M, Takahashi T, Okoshi S, Kawai H, Mita Y, Waguri N, Aoyagi Y. Interferon can block telomere erosion and in rare cases result in hepatocellular carcinoma development with telomeric repeat binding factor 1 overexpression in chronic hepatitis C. *Clin Cancer Res* 2003; **9**: 5264-5270

22 **Ueda H**, Ullrich SJ, Gangemi JD, Kappel CA, Ngo L, Feitelson MA, Jay G. Functional inactivation but not structural mutation of p53 causes liver cancer. *Nat Genet* 1995; **9**: 41-47

23 **McCaffrey AP**, Nakai H, Pandey K, Huang Z, Salazar FH, Xu H, Wieland SF, Marion PL, Kay MA. Inhibition of hepatitis B virus in mice by RNA interference. *Nat Biotechnol* 2003; **21**: 639-644

24 **Song E**, Lee SK, Wang J, Ince N, Ouyang N, Min J, Chen J, Shankar P, Lieberman J. RNA interference targeting Fas protects mice from fulminant hepatitis. *Nat Med* 2003; **9**: 347-351

25 Whither RNAi? *Nat Cell Biol* 2003; **5**: 489-490

26 **Birmingham A**, Anderson EM, Reynolds A, Ilsley-Tyree D, Leake D, Fedorov Y, Baskerville S, Maksimova E, Robinson K, Karpilow J, Marshall WS, Khvorova A. 3' UTR seed matches, but not overall identity, are associated with RNAi off-targets. *Nat Methods* 2006; **3**: 199-204

27 **Maeda K**, Okubo K, Shimomura I, Funahashi T, Matsuzawa Y, Matsubara K. cDNA cloning and expression of a novel adipose specific collagen-like factor, apM1 (AdiPose Most abundant Gene transcript 1). *Biochem Biophys Res Commun* 1996; **221**: 286-289

28 **Yanai I**, Benjamin H, Shmoish M, Chalifa-Caspi V, Shklar M, Ophir R, Bar-Even A, Horn-Saban S, Safran M, Domany E, Lancet D, Shmueli O. Genome-wide midrange transcription profiles reveal expression level relationships in human tissue specification. *Bioinformatics* 2005; **21**: 650-659

29 **Prasad NB**, Biankin AV, Fukushima N, Maitra A, Dhara S, Elkahloun AG, Hruban RH, Goggins M, Leach SD. Gene expression profiles in pancreatic intraepithelial neoplasia reflect the effects of Hedgehog signaling on pancreatic ductal epithelial cells. *Cancer Res* 2005; **65**: 1619-1626

30 **Onda M**, Emi M, Nagai H, Nagahata T, Tsumagari K, Fujimoto T, Akiyama F, Sakamoto G, Makita M, Kasumi F, Miki Y, Tanaka T, Tsunoda T, Nakamura Y. Gene expression patterns as marker for 5-year postoperative prognosis of primary breast cancers. *J Cancer Res Clin Oncol* 2004; **130**: 537-545

31 **Kang HC**, Kim IJ, Park JH, Shin Y, Ku JL, Jung MS, Yoo BC, Kim HK, Park JG. Identification of genes with differential expression in acquired drug-resistant gastric cancer cells using high-density oligonucleotide microarrays. *Clin Cancer Res* 2004; **10**: 272-284

32 **Scott BJ**, Qutob S, Liu QY, Ng CE. APM2 is a novel mediator of cisplatin resistance in a variety of cancer cell types regardless of p53 or MMR status. *Int J Cancer* 2009; **125**: 1193-1204

33 **Norton PA**, Gong Q, Mehta AS, Lu X, Block TM. Hepatitis B virus-mediated changes of apolipoprotein mRNA abundance in cultured hepatoma cells. *J Virol* 2003; **77**: 5503-5506

34 **Tong A**, Wu L, Lin Q, Lau QC, Zhao X, Li J, Chen P, Chen L, Tang H, Huang C, Wei YQ. Proteomic analysis of cellular protein alterations using a hepatitis B virus-producing cellular model. *Proteomics* 2008; **8**: 2012-2023

35 **Niu D**, Sui J, Zhang J, Feng H, Chen WN. iTRAQ-coupled 2-D LC-MS/MS analysis of protein profile associated with HBV-modulated DNA methylation. *Proteomics* 2009; **9**: 3856-3868

36 **Narayan R**, Gangadharan B, Hantz O, Antrobus R, García A, Dwek RA, Zitzmann N. Proteomic analysis of HepaRG cells: a novel cell line that supports hepatitis B virus infection. *J Proteome Res* 2009; **8**: 118-122

37 **Tong A**, Gou L, Lau QC, Chen B, Zhao X, Li J, Tang H, Chen L, Tang M, Huang C, Wei YQ. Proteomic profiling identifies aberrant epigenetic modifications induced by hepatitis B virus X protein. *J Proteome Res* 2009; **8**: 1037-1046

S- Editor Wu X **L- Editor** Roemmele A **E- Editor** Wu X

CLINICAL STUDY

Formula to Predict Platelet Count after Partial Splenic Arterial Embolization in Patients with Hypersplenism

Akihiko Osaki, MD, Takeshi Suda, MD, Nobuo Waguri, MD, Toru Ishikawa MD, Takeshi Yokoo, MD, Kenya Kamimura, MD, Yasushi Tamura, MD, Masaaki Takamura, MD, Masato Igarashi, MD, Hirokazu Kawai, MD, Satoshi Yamagiwa, MD, and Yutaka Aoyagi, MD

ABSTRACT

Purpose: To establish a formula to guide appropriate embolization volume for postprocedural platelet gain following partial splenic arterial embolization (PSE) for hypersplenism.

Materials and Methods: The hepatic volume (Vh) and splenic volume (Vsp) were measured by using 2-mm-thick computed tomography images before and after PSE in 20 patients with various chronic liver diseases. A formula was derived from the relationship between the platelet count increase ratio (dPlt%) and the organ volumes, which was then evaluated in another cohort.

Results: After an embolization of a median of 72.1% of the spleen (interquartile range, 38.2%–93.8%), the dPlt% was 67.7% ± 40.0 and significantly correlated with the increasing ratio of Vh to Vsp ($P = .019$, $\rho = 0.52$). Because the difference in Vh/Vsp ratio after PSE was significantly correlated with the spleen embolization ratio (eVsp%; $P = .0003$, $\rho = 0.72$), the estimated dPlt% could be derived from the Vh/Vsp ratio before PSE and the eVsp%. The estimated dPlt% was significantly correlated with the actual dPlt% ($P = .0003$, $\rho = 0.72$). When the formula was evaluated in another cohort of 14 cases, another strict correlation was observed ($P < .0001$, $\rho = 0.92$).

Conclusions: These data suggest that platelet count after PSE can be predicted before the procedure by using the Vh/Vsp ratio and the anticipated spleen embolization volume. The use of such a prediction can prevent too much or too little embolization, thereby leading to an improvement in the risk/return trade-off in PSE.

ABBREVIATIONS

d(Vh/Vsp) = difference between hepatic/splenic volume ratios before partial splenic arterial embolization and at stabilized phase after partial splenic arterial embolization, d(Vh/Vsp)% = percentage difference between hepatic/splenic volume ratios before partial splenic arterial embolization and at stabilized phase after partial splenic arterial embolization, dPlt% = platelet count increase ratio, eVsp = spleen embolization volume, eVsp% = spleen embolization ratio, HCV = hepatitis C virus, ICG = indocyanine green, IQR = interquartile range, PSE = partial splenic arterial embolization, Vh = hepatic volume, Vsp = splenic volume

Patients with chronic liver diseases frequently experience thrombocytopenia in proportion to the severity of their liver disease (1,2), which prevents the application of crucial treatments. The administration of pegylated interferon with ribavirin is central for the eradication of the hepatitis C virus (HCV) but readily diminishes the platelet count. If the platelet count is less than $10 \times 10^4/\mu L$ at the beginning of treatment, patients often cannot complete the recommended dose and duration of therapy. Hepatocellular carcinoma predominantly results from cirrhotic liver and requires the

From the Division of Gastroenterology and Hepatology (A.O., T.Y., K.K., Y.T., M.T., M.I., H.K., S.Y., Y.A.), Graduate School of Medical and Dental Sciences, Niigata University, 1-757 Asahimachi-dori, Chuo-ku, Niigata, Niigata 951-8122, Japan; Division of Gastroenterology and Hepatology (T.S.), Niigata University Medical and Dental Hospital; Division of Gastroenterology and Hepatology (N.W.), Niigata City General Hospital; and Division of Gastroenterology and Hepatology (T.I.), Saiseikai Niigata Second Hospital, Niigata, Japan. Received December 10, 2011; final revision received February 28, 2012; accepted March 14, 2012. **Address correspondence to** T.S.; E-mail: suda@med.niigata-u.ac.jp

None of the authors have identified a conflict of interest.

J Vasc Interv Radiol 2012; 23:900–907

http://dx.doi.org/10.1016/j.jvir.2012.03.008

administration of anticancer agents, especially when the disease advances beyond manageability by locoregional treatments such as surgical resection or radiofrequency ablation (3–5). The thrombocytopenia associated with cirrhosis, however, restricts the use of bone marrow suppressive drugs in many cases.

Cirrhotic thrombocytopenia is a multifactorial condition (6). Increased sequestration of platelets by the enlarged spleen, reduced platelet production, and accelerated platelet turnover all contribute to the condition. Partial splenic arterial embolization (PSE) has been widely adopted as an effective alternative to splenectomy (7) because of the results of Maddison's 1973 report (8). The reduction of splenic volume (Vsp) can diminish platelet sequestration and reduce rapid turnover. Several lines of evidence clearly indicate that PSE significantly augments platelet numbers in the hypersplenic state resulting from chronic liver diseases (7,9–12). However, a correlation between platelet count and infarction volume is controversial. Noguchi et al (9) and Hayashi et al (10) separately reported a significant correlation between the spleen infarction ratio and an increased platelet count, whereas Han et al (12) did not reveal a significant correlation. In addition, larger infarction volumes are a potential risk factor for complications (13), including the formation of lethal pyogenic abscesses (14). Although various investigations have been conducted to determine how to best avoid unnecessary or insufficient embolization when carrying out PSE, a way of practically predicting PSE efficacy has not been achieved.

The goal of this study was to establish a formula for estimating the platelet count after PSE. Because the incidence and intensity of cirrhotic thrombocytopenia increase in association with the severity of liver diseases (1,2,15), we hypothesized that Vsp and hepatic volume (Vh) may reflect the destruction and production of platelets, respectively. Here, we report a formula that consists of Vsp and Vh, and the clinical benefits of feasibly predicting the platelet count are discussed.

MATERIALS AND METHODS

Patients

The relationship between clinicopathologic data and platelet count augmentation was retrospectively evaluated in 34 consecutive cases of PSE between July 2006 and January 2011. The patient characteristics are summarized in **Table 1**, including three cases in which PSE was performed twice (for which each procedure was analyzed independently as cases 4 and 22, 6 and 7, and 15 and 22). PSE was performed to increase the platelet count and/or to alleviate esophageal or gastric varices. Balloon-occluded retrograde transvenous obliteration or endoscopic variceal ligation was concomitantly carried out in eight cases. To avoid an underestimation of the efficacy of PSE on augmenting the platelet count, interferon administration or chemotherapy was not initiated until the fluctuation of the platelet count after PSE was stabilized to within 20% in 1 month. Adverse events were categorized according to the clinical practice guidelines of the Society of Interventional Radiology (16). Major adverse events were defined as those necessitating an increased level of care, major therapy, or prolonged hospitalization, as well as those resulting in permanent sequelae or death. Minor adverse events were defined as those requiring nominal therapy or observation only. In addition to the 34 cases of PSE, 17 consecutive patients with cirrhosis were subjected to liver volumetry; therefore, the relationship between Vh and functional liver reserve was evaluated in 51 patients. The Child–Pugh score was not evaluated in five cases because these patients regularly took anti–vitamin K drugs. The disappearance rate of indocyanine green (ICG) was calculated to represent the slope of an exponential equation. A dose of 0.5 mg/kg ICG was intravenously injected on a morning at rest after fasting more than 8 hours; blood samples were drawn before the injection and 5, 10, and 15 min after the injection. The ICG plasma elimination data were fitted to a monoexponential equation by using a log-linear least-squares method. Informed consent was obtained from each patient, and the study protocol conformed to the ethical guidelines of the 2008 Declaration of Helsinki, as reflected in the prior approval by the Niigata University Graduate School of Medical and Dental Sciences Human Research Committee.

Partial Splenic Arterial Embolization

Oral administration of antibiotics (levofloxacin hydrate; Daiichi Snakyo, Tokyo, Japan) and probiotics was initiated 3 days before PSE. A 5-F catheter, such as a FANSAC catheter (Terumo Clinical Supply, Gifu, Japan), was introduced into the celiac artery from the femoral artery and advanced into the splenic artery as far as possible. A 2.2–2.7-F catheter, such as a Sniper 2 catheter (Terumo Clinical Supply), was coaxially advanced further into a branch of the splenic artery, and the tip was placed where embolization was desired. Computed tomography (CT) images were obtained from splenic arteriography before and/or after the procedure, and the embolizing volume was calculated. Until the embolization spanned a desired volume, the procedure was repeated by injecting gelatin sponge cubes of approximately 3 mm^3 (Astellas Pharma, Tokyo, Japan) suspended in contrast medium containing antibiotics (imipenem hydrate/cilastatin sodium; MSD K.K., Tokyo, Japan) or metallic coils (C-Stopper, 60–100 mm; Piolax, Kanagawa, Japan). Antibiotics were systemically administered for at least 3 days after PSE and continued depending on the patient's condition.

CT Study

A helical CT scan was performed with a 2-mm collimation by using one of following scanners: SOMATOM Sensation 16, Definition Flash, Definition/Sensation 64 (Siemens, Erlangen, Germany); LightSpeed VCT (GE Healthcare Japan, Tokyo, Japan); or Aquilion 64 (Toshiba, Tokyo, Japan). To

Table 1. Patient Characteristics and Volume Data

Case No.	Sex	Diagnosis	C–P Score	Aim	Vsp before PSE (mL)	Vh before PSE (mL)	eVsp (mL)	Vsp after PSE (mL)	Vh after PSE (mL)	Platelets ($\times 10^4/\mu L$) Before PSE	Platelets ($\times 10^4/\mu L$) After PSE
1	F	HCV	5	IFN	526.0	1,620.0	474.0	108.8	1,727.1	5.9	8.6
2	M	ALC	5	GV	496.0	1,182.4	413.0	141.8	1,202.4	7.3	13.6
3	F	PBC	6	B-RTO	508.4	905.3	444.5	69.5	1,033.9	9.3	22.1
4	F	HCV	5	IFN	408.3	744.6	263.0	165.0	790.9	5.5	9.7
5	M	HCV	8	Cx	336.3	802.0	169.8	214.2	833.0	5.1	7.1
6	M	HBV	5	EVL	962.0	1,006.2	397.6	647.7	961.8	5.0	5.2
7 (6)	M	HBV	5	EVL	688.4	909.7	422.8	439.1	1,025.5	5.1	8.8
8	F	IPH	6	EV	163.2	883.6	96.9	81.9	955.8	13.5	15.7
9	F	AIH	7	EVL	642.2	1,053.6	245.4	404.6	944.1	6.5	9.2
10	F	Alcohol	6	B-RTO	256.5	1,104.4	178.5	87.1	1,003.7	9.1	9.7
11	M	HCV	6	IFN	384.8	1,065.4	268.1	185.8	1,104.2	5.0	10.2
12	F	HCV	7	IFN	358.3	697.7	298.1	109.9	797.7	5.3	10.6
13	M	EHO	5	GV	353.5	886.0	263.4	76.7	784.4	11.4	17.9
14	F	HCV	6	IFN	498.3	907.3	467.4	66.4	959.3	5.3	10.0
15	M	HCV	11	B-RTO	228.9	978.1	159.4	152.8	1,501.7	3.9	4.9
16	F	EHO	6	GV	1,318.9	1,135.9	882.7	555.1	1,225.0	10.8	22.2
17	F	HBV	5	B-RTO	374.4	905.0	294.3	91.4	932.6	9.8	22.4
18	M	HCV	6	GV, EV	291.0	2,011.1	226.7	161.9	1,733.0	11.1	19.3
19	F	HCV	5	IFN	256.5	1,044.7	196.5	83.4	1,021.9	5.4	11.4
20	M	HCV	5	EV	1,327.9	2,115.9	1,118.1	417.3	1,849.4	5.6	14.8
21	M	HCV	6	IFN	823.2	1,045.2	327.6	ND	ND	3.5	5.1
22 (4)	F	HCV	5	IFN	165.0	790.9	132.0	ND	ND	9.7	11.9
23	F	HCV	7	B-RTO	412.3	1,079.9	328.6	ND	ND	6.7	14.8
24	M	HCV	5	IFN	269.7	1,292.2	250.3	ND	ND	7.7	15.6
25 (15)	M	HCV	7	IFN	152.8	1,501.7	113.6	ND	ND	4.9	5.7
26	M	EHO	5	GV	922.9	1,527.5	624.7	ND	ND	10.9	18.6
27	F	HCV	7	Cx	277.6	626.1	258.2	ND	ND	5.7	13.4
28	M	HCV	8	Cx	1,014.3	1,382.6	871.3	ND	ND	4.0	14.5
29	M	HCV	5	EV	799.6	1,047.2	704.4	ND	ND	3.7	11.9
30	F	IPH	5	SpA	904.0	1,438.7	596.6	ND	ND	7.5	14.4
31	M	Alcohol	6	GV	524.6	969.6	317.9	ND	ND	5.7	9.1
32	M	HCV	5	IFN	194.2	1,315.7	160.2	ND	ND	9.2	13.7
33	M	HBV	6	Cx	980.7	1,384.2	742.6	ND	ND	5	10.2
34	F	HCV	5	Cx	720.0	1,406.7	452.1	ND	ND	4	6.2

Note.—AIH = autoimmune hepatitis, B-RTO = balloon-occluded retrograded obliteration, C–P = Child–Pugh score, Cx = preparation for systemic chemotherapy, EHO = extrahepatic portal vein obstruction, EV = esophageal varices, EVL = endoscopic variceal ligation, eVsp = embolized splenic volume, GV = gastric varices, HBV = hepatitis B virus, HCV = hepatitis c virus, IFN = interferon therapy for HCV eradication, IPH = idiopathic portal hypertension, ND = not determined, PBC = primary biliary cirrhosis, SpA = splenic artery aneurysm, Vh = hepatic volume, Vsp = splenic volume.

A case number in parenthesis indicates an original case number for the cases attempting the second PSE.

improve the contrast, 1.62 mL/kg of iodine contrast medium at a concentration of 370 mg/mL was injected over a period of 30 seconds from a peripheral vein, and CT images were obtained 20 seconds after the CT attenuation exceeded 200 HU in the aorta, 30 seconds after the initiation of the first phase, and 180 seconds after starting the injection of contrast medium. For CT during splenic arteriography, contrast medium at a concentration of 150 mg/mL was injected at a speed of 1 mL/s over the duration of the scan, which was started with a delay of 10 seconds. Conventional CT scans were performed before PSE (median, 5.5 d; interquartile range [IQR], 0–235 d) and immediately after or within 2 weeks of PSE. In cases 1–20 in **Table 1**, additional CT images were obtained after the platelet count had stabilized (median, 137 d; IQR, 41–339 d), and in the other 14 cases, cases 21–34 in **Table 1**, which served as a testing cohort, no CT study was performed in the chronic phase. The interval between the CT scan and platelet count evaluation after PSE was no more than 1 month (median, 0 d; IQR, 0–26 d).

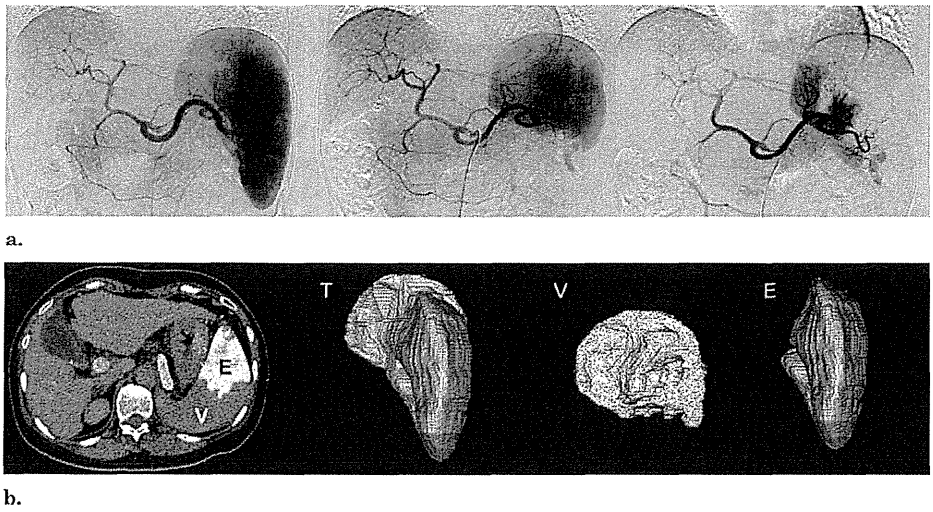

Figure 1. Representative PSE images. **(a)** Representative celiac arteriograms show PSE repeated as observed from left to right (before, first, and second) by confirming the embolized area. **(b)** CT images were obtained during splenic arteriography before the first PSE by using a microcatheter tip placed where the PSE would be performed. After the entire embolized and preserved spleen had been traced in the CT images, the three-dimensional voxel data were obtained and used to calculate the volume. *T*, total spleen; *V*, viable; *E*, embolized.

Volumetry of Liver and Spleen

Representative areas of the liver or spleen were manually segmented under a window width of 1,000 and a window level of 250. The volume between the areas that were defined by manual segmentation was automatically calculated by using Aquarius Net Station software (version 1.5; TeraRecon, Tokyo, Japan), and the number of pixels with CT attenuation greater than −500 HU was counted. With $1 \times 1 \times 2$ mm^3 for each pixel as a voxel, the target Vh or Vsp was then calculated. The Vh was quantified before PSE or other invasive treatments and excluded any vessels larger than the first branch of the portal vein. The spleen embolizing volume (eVsp) was divided by Vsp to calculate a spleen embolization ratio (eVsp%). The difference between Vh/Vsp before PSE and Vh/Vsp at the stabilized phase after PSE was defined as d(Vh/Vsp), and the percentage of d(Vh/Vsp) versus Vh/Vsp before PSE was defined as d(Vh/Vsp)%.

Statistical Analyses

The eVsp% or platelet count value was compared with various factors by using a Friedman test followed by Dunn multiple-comparison test for a comparison of three groups and a Wilcoxon matched-pairs signed-rank test for a comparison of two groups. The Vh values of the Child-Pugh A and B stages were compared by using a Mann-Whitney test. The correlations were quantified by calculating the Spearman correlation coefficient. A multivariate analysis was performed using a stepwise model building procedure based on a significance value of 0.05 for both inclusion and exclusion of predicting factors. All analyses were performed by using GraphPad Prism 5 software (GraphPad Software, La Jolla, California) except for the multivariate analysis, which was performed with PASW statistics (version 17.0; SPSS, Chicago, Illinois). A two-sided *P* value less than .05 was considered statistically significant.

RESULTS

Safety and Efficacy of PSE

PSE was performed in 34 cases (**Fig 1**). Initially, 20 cases, listed as cases 1–20 in **Table 1**, were evaluated as a cohort to deduce a formula that predicts the platelet count after PSE. As shown in **Figure 2**, median eVsp% was calculated by CT volumetry to be 72.1% (IQR, 38.2%–93.8%) immediately after the procedure, and eVsp% significantly decreased to a median of 25.2% (IQR, 7.2%–66.9%) 2 months or more after PSE. However, eVsp% did not significantly change within 2 weeks of PSE in 17 cases, among which median eVsp% was 76.6% (IQR, 38.4%–93.8%). The median platelet count significantly increased from $5.8 \times 10^4/\mu$L (IQR, 3.9–13.5 $\times 10^4/\mu$L) before PSE to $10.4 \times 10^4/\mu$L (IQR, 4.9–22.4 $\times 10^4/\mu$L) by the post-PSE stable period (**Fig 2b**). The median Vh values were 992 mL (IQR, 698–2,116 mL) and 1,013 mL (IQR, 784–1,849 mL) before PSE and at the post-PSE platelet-stable phase, respectively; these values are not significantly different ($P = .47$). No major adverse events were recorded. Left upper flank pain and pyrexia generally developed but were well controlled with a regular oral dose of nonsteroidal antiinflammatory drugs.

Correlation of Vh and Vsp with Platelet Count after PSE and Functional Liver Reserve

Under normal conditions, platelets are mainly destroyed in the spleen. According to the assumption that the platelet count may be defined by Vsp, whether there is a correlation between Vsp and the platelet count after PSE was evaluated. The platelet count did not correlate with Vsp after PSE, as demonstrated in **Figure 3a** ($P = .15$, $\rho = -0.34$). On the contrary, Vh was associated with functional liver reserve. When Vh was compared